Structural characterization of the human respiratory syncytial virus fusion protein core

Xun Zhao, Mona Singh, Vladimir N. Malashkevich, and Peter S. Kim*

Howard Hughes Medical Institute, Whitehead Institute for Biomedical Research, Department of Biology, Massachusetts Institute of Technology, Nine Cambridge Center, Cambridge, MA 02142

Contributed by Peter S. Kim, October 20, 2000

Human respiratory syncytial virus (HRSV) is a major cause of a number of severe respiratory diseases, including bronchiolitis and pneumonia, in infants and young children. The HRSV F protein, a glycoprotein essential for viral entry, is a primary target for vaccine and drug development. Two heptad-repeat regions within the HRSV F sequence were predicted by the computer program LEARNCOIL-VMF. These regions are thought to form trimer-of-hairpins–like structures, similar to those found in the fusion proteins of several enveloped viruses. The hairpin structure likely brings the viral and cellular membranes into close apposition, thereby facilitating membrane fusion and subsequent viral entry. Here, we show that peptides, denoted HR-N and HR-C, corresponding to the heptad-repeat regions from the N-terminal and C-terminal segments of the HRSV F protein, respectively, form a stable α-helical trimer of heterodimers. The HRSV N/C complex was crystallized and its x-ray structure was determined at 2.3-Å resolution. As anticipated, the complex is a six-helix bundle in which the HR-N peptides form a three-stranded, central coiled coil, and the HR-C peptides pack in an antiparallel manner into hydrophobic grooves on the coiled-coil surface. There is remarkable structural similarity between the HRSV N/C complex and the fusion protein core of other viruses, including HIV-1 gp41. In addition, earlier work has shown that HRSV HR-C peptides, like the HIV-1 gp41 C peptides, inhibit viral infection. Thus, drug discovery and vaccine development strategies aimed at inhibiting viral entry by blocking hairpin formation may be applied to the inhibition of HRSV.

x-ray crystallography | membrane fusion | pneumovirus

Human respiratory syncytial virus (HRSV), a member of the pneumovirus subfamily of the Paramyxoviridae family (1), is a leading cause of severe respiratory infections in infants and young children worldwide (2). A safe and effective HRSV vaccine is not yet available, so it is important to pursue potential therapeutic measures against HRSV infection.

HRSV carries three surface glycoproteins: F, G, and SH (1). The HRSV F protein is an attractive target for drug and vaccine development as it is essential for viral entry, is highly conserved, and is the major virus neutralization antigen (1). In contrast, the G protein is highly variable among different strains of HRSV (3), and the SH protein has been found to be dispensable for virus growth (4).

The F protein is synthesized as a 67-kDa precursor (denoted F0) that is processed by proteolytic cleavage to yield two disulfide-linked subunits: F1 and F2 (Fig. 1). The fusion peptide region, a hydrophobic/glycine-rich segment that inserts into the target cellular membrane during the fusion process, is located at the N terminus of the F1 subunit (1). The transmembrane segment is close to the C terminus of the F1 subunit. Adjacent to both the fusion peptide and transmembrane segments are two regions containing 4,3-hydrophobic heptad repeats (HR), a sequence motif suggestive of coiled-coil structures (5–7). These regions are denoted HR-N and HR-C, respectively, and are separated by an intervening domain of ≈270 residues. In general, the arrangement of these structural elements in the F1 protein is highly conserved among the Paramyxoviridae family (8).

Previous studies with viral fusion proteins (ref. 7 and references therein), including hemagglutinin of influenza (9, 10), TM subunit of Moloney murine leukemia virus (11), gp41 of HIV-1 and simian immunodeficiency virus (12–17), GP2 of Ebola (18, 19), gp21 of human T cell leukemia virus type 1 (20), and F1 of simian parainfluenza virus 5 (SV5) (21), suggest that HR-N and HR-C form trimeric hairpin-like structures, with the HR-C regions packing in an antiparallel manner against the inner coiled coil formed by the HR-N regions. The likely role of the hairpin structure is to facilitate apposition of the viral and cellular membranes by bringing the fusion peptide, which inserts into the cellular membrane, close to the transmembrane segment, which is anchored in the viral membrane. Hence, the trimer-of-hairpins structure presumably corresponds to the fusion-active state, distinct from the native (nonfusogenic) state. But whether hairpin formation precedes the actual membrane-fusion event or occurs simultaneously with fusion is unknown.

There is extensive biochemical evidence to suggest that viral fusion proteins undergo conformational changes when activated (22, 23). Earlier work on the HIV-1 fusion protein gp41 led to a model for viral membrane fusion (Fig. 2) in which gp41 exists in at least three different conformations: (*i*) the native (nonfusogenic) form, where the fusion peptide and HR-N region are inaccessible, (*ii*) the prehairpin intermediate, where the HR-N region is exposed and the fusion peptide is projected into the target cellular membrane, and (*iii*) the fusogenic hairpin form, where the HR-N and HR-C regions associate and bring the viral and the cellular membranes together to facilitate fusion (24).

Agents that prevent these conformational changes by stabilizing the native or intermediate states are expected to prevent fusion activation and thus block viral entry. In the case of HIV-1 gp41, peptides corresponding to the HR-C region of gp41, referred to as C peptides, can effectively inhibit infection (24). One such C peptide is in clinical trials and shows antiviral activity in humans (25). C peptides function in a dominant-negative manner by binding to the transiently exposed coiled coil in the prehairpin intermediate and consequently blocking the formation of the fusion-active hairpin structures (24).

A similar approach may be effective in identifying inhibitors of HRSV infection. HR-C regions from HRSV have been shown to inhibit viral infection and thus provide evidence that the F protein also may display the prehairpin intermediate conformation (26). Analogous to the HIV-1 C peptides, these HRSV

Abbreviations: HRSV, human respiratory syncytial virus; HR, heptad repeat; SV5, simian parainfluenza virus 5.

Data deposition: The atomic coordinates have been deposited in the Protein Data Bank, www.rcsb.org (PDB ID code 1G2C).

*To whom reprint requests should be addressed. E-mail: kimadmin@wi.mit.edu.

The publication costs of this article were defrayed in part by page charge payment. This article must therefore be hereby marked "*advertisement*" in accordance with 18 U.S.C. §1734 solely to indicate this fact.

Article published online before print: *Proc. Natl. Acad. Sci. USA*, 10.1073/pnas.260499197. Article and publication date are at www.pnas.org/cgi/doi/10.1073/pnas.260499197

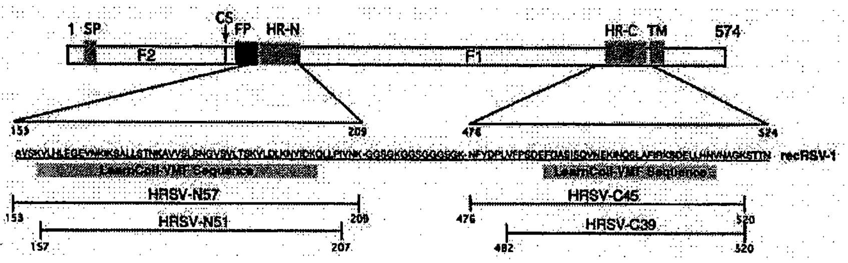

Fig. 1. Schematic diagram of the HRSV F protein sequence. F1 and F2 are formed after proteolytic cleavage of the precursor F0. The signal peptide (SP), the cleavage site (CS), the putative fusion peptide (FP), the N-terminal HR (HR-N) region, the C-terminal HR (HR-C) region, and the transmembrane segment (TM) within the amino acid sequence of the recombinant recRSV-1 construct are indicated. The HR-N and HR-C regions predicted by LEARNCOIL-VMF are represented by shaded boxes. Protease-resistant fragments from trypsin (HRSV-N57 and HRSV-C45) and proteinase K (HRSV-N51 and HRSV-C39) cleavage are indicated.

HR-C peptides likely act in a dominant-negative manner to prevent the formation of final fusion-active structures, thereby inhibiting viral entry.

To verify that the HRSV F1 protein core indeed forms a trimer-of-hairpins structure and to provide a structural basis for the development of fusion inhibitors, we characterized the interaction of the two HR regions of HRSV F1 protein. We identified two peptides, HRSV-N57 and HRSV-C45, which correspond to the HR-N and HR-C regions of HRSV F1 protein, respectively, that form a stable trimer of heterodimers. This result is consistent with recent reports that indicate the HR-N and HR-C regions from HRSV associate to form an α-helical trimer of heterodimers (27, 28). The HRSV-N57/C45 complex characterized here was crystallized, and its x-ray structure was determined to 2.3-Å resolution. The structure confirms the similarity between the HRSV F1 protein core and several other viral fusion proteins, including HIV-1 gp41, suggesting that methods for discovery of potential therapeutics and prophylactics developed against HIV-1 gp41 also might apply to the HRSV F1 protein.

Materials and Methods

Gene Construction and Purification of recRSV-1. Using optimal codons for *Escherichia coli* expression (29), a synthetic gene sequence denoted recRSV-1 was constructed that encodes residues 153–209 and 476–524 of HRSV (strain RSS-2; Swiss-Prot accession no. P11209), connected by a glycine-rich linker (Fig. 1). A factor Xa cleavage site was incorporated upstream of the HRSV coding sequence. The constructed gene was inserted into the *Bam*HI–*Hin*dIII restriction site of the hexahistidine expression vector pQE9 (Qiagen, Chatsworth, CA). The resulting plasmid, denoted pRSV-1, was transformed into *E. coli* XL1-Blue competent cells for protein expression. Cells were grown in Luria–Bertani medium to an optical density of 0.6 at 600 nm. Protein expression then was induced with 1 mM isopropyl-β-D-thiogalactopyranoside, and cells were harvested after 3 h.

Cells were lysed in 6 M guanidine-HCl, and the lysate was clarified by centrifugation. The recombinant protein was purified by nickel-nitrilotriacetic acid metal-affinity chromatography, followed by reverse-phase HPLC (Waters) using a Vydac C18 preparative column (Vydac, Hesperia, CA) with a water/acetonitrile gradient of 0.1%/min in the presence of 0.1% trifluoroacetic acid. The mass of the purified protein was verified by mass spectrometry on a Voyager Elite matrix-assisted laser desorption ionization-time of flight mass spectrometer (PerSeptive Biosystems, Framingham, MA). The protein was lyophilized and resuspended in ultrapure water and dialyzed against factor Xa cleavage buffer (50 mM Tris·HCl, pH 8.0/100 mM NaCl/2 mM $CaCl_2$). To remove the His tag, factor Xa was added at a 1:500 wt/wt ratio of protease to tagged protein, and the reaction was incubated for 2 days at room temperature. The cleavage mixture then was purified by reverse-phase HPLC on a Vydac C18 preparative column. Peak fractions containing recRSV-1 were verified by mass spectrometry and lyophilized.

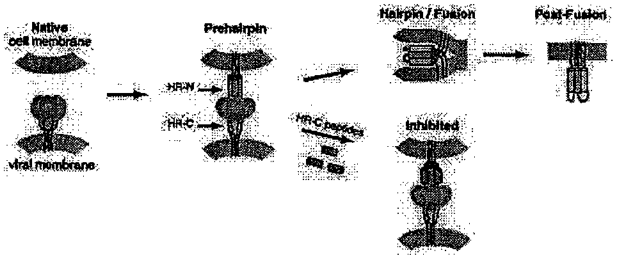

Fig. 2. A model for virus–cell membrane fusion (24). The model shown is based primarily on studies of the HIV-1 gp41-mediated membrane fusion process. The HRSV F protein likely undergoes similar conformational changes. In the native state, the fusion peptide (not shown) is inaccessible. Upon activation, the fusion protein undergoes a conformational change to the prehairpin intermediate, in which the fusion peptide (red lines) is inserted into the target-cell membrane, and the HR-N peptide region (gray) is a trimeric coiled coil. The HR-C peptide region (yellow) has not yet associated with the N peptide coiled coil. This intermediate is vulnerable to HR-C peptide inhibition (*Lower*, inhibitory peptides shown in orange). The prehairpin intermediate resolves to the fusion-active hairpin structure when the HR-C peptide region binds to the HR-N peptide coiled coil and adopts a helical conformation. This rearrangement results in membrane apposition. Whether hairpin formation precedes the actual membrane-fusion event or occurs simultaneously with fusion is unknown. Figure was adapted from Chan and Kim (24).

Proteolysis. All proteolysis reactions were performed with 1 mg/ml protein and 0.1 mg/ml protease in PBS, pH 7.4, at room temperature and quenched with 2 mM PMSF (final concentration). Proteolysis samples were analyzed by reverse-phase HPLC connected to an LCQ electrospray mass spectrometer (Finnigan-MAT, San Jose, CA). Fragments were assigned by matching observed masses with a list of possible fragment masses predicted by the computer program FRAGMENT MASS (E. Wolf and P. S. Kim, http://www.wi.mit.edu/kim/computing.html). Assigned fragments were within 1 Da of their predicted values.

CD Spectroscopy. CD spectra were measured at 10 μM protein concentration in PBS buffer with an AVIV 62 DS spectrometer (Aviv Associates, Lakewood, NJ) as described (30). Protein concentrations were determined by absorbance at 280 nm in 20 mM phosphate-buffered 6 M guanidine-HCl (pH 6.5) (31).

Sedimentation Equilibrium Analysis. Sedimentation equilibrium analysis was performed on a Beckman XLA-90 analytical ultracentrifuge (Beckman Instruments) at 15,000 rpm and 20,000 rpm, and data were collected after spinning for 18 h at 20°C.

Three protein samples at concentrations of 10, 50, and 100 μM were spun, following dialysis against PBS buffer overnight. Data analyses were performed as described (32).

Purification, Crystallization, and Structure Determination of the HRSV-N57/C45 Trimer. The HRSV-N57 and HRSV-C45 peptides were generated by trypsin digestion of recRSV-1 protein and purified to homogeneity by reverse-phase HPLC on a Vydac C18 preparative column. The purified HRSV peptides were lyophilized and dissolved in water and 10 mM Tris·HCl (pH 8.5), respectively. Equimolar amounts of HRSV-N57 and HRSV-C45 were mixed, and the complex was separated from the free peptide and aggregated species by gel filtration on a Sephacryl S-100 HR column (Amersham Pharmacia) in buffer (10 mM Tris·HCl, pH 8.5/50 mM NaCl). The purified HRSV-N57/C45 complex was concentrated to 10 mg/ml.

Crystals were obtained by using the hanging drop method by equilibrating 2-μl drops (protein solution mixed 1:1 with reservoir solution) against a reservoir solution containing 24–26% polyethylene glycol 4000/200 mM Tris·HCl, pH 8.5/300 mM Li_2SO_4. The crystals belong to the space group *P1* (a = 67.9 Å, b = 71.5 Å, c = 76.5 Å, α = 81.3°, β = 73.8°, γ = 60.7°). There are four trimers per asymmetric unit that give rise to a solvent content of ≈46%. For data collection, crystals were directly mounted in nylon loops (Hampton Research, Riverside, CA) from the drop and flash-frozen in liquid nitrogen. Diffraction data were collected at 100 K at the Howard Hughes Medical Institute Beamline X4A at Brookhaven National Laboratory, Brookhaven, NY, using a Quantum-4 CCD detector. Diffraction intensities were integrated by using DENZO and SCALEPACK software (33) and reduced to structure factors with the program TRUNCATE from the CCP4 program suite (34). The structure of the HRSV-N57/C45 complex was solved by molecular replacement with the program AMORE (47). A polyserine model derived from the SV5 N1/C1 trimer (21) was used as a search model. Initially, only three molecules per asymmetric unit were found. After applying solvent flattening, histogram matching, and 9-fold noncrystallographic averaging with the program DM (35), the electron density map was interpretable in most regions. Three HRSV-N57/C45 trimer molecules were built into the density using the program O (36). After a few cycles of refinement, the R_{free} value remained high, and the existence of unassigned continuous density was suggestive of a fourth molecule. Molecular replacement with a partially refined HRSV-N57/C45 trimer molecule readily located the fourth trimer in the unit cell. Crystallographic refinement of the structure (Table 1) was done with the CNS programs (37) (reflections beyond 2.3 Å were not used due to poor quality). Noncrystallographic symmetry restraints were applied during the first few cycles of refinement but then were removed and not used in the final refinement. The quality of coordinates was examined by PROCHECK (38). No residues were in disallowed regions, and 94.5% were in the most favored regions of the Ramachandran plot.

Results

HRSV-N57 and HRSV-C45 Peptides Form a Stable Trimeric α-Helical Complex. LEARNCOIL-VMF, a program for identifying coiled-coil-like regions in viral fusion proteins, predicts such regions in the HRSV F1 protein (7). The first region (residues 156–201) is near the putative fusion peptide, and the second region (residues 488–516) is adjacent to the transmembrane segment (Fig. 1).

To study the regions predicted by LEARNCOIL-VMF, we constructed a recombinant protein, recRSV-1, corresponding to residues 153–209 and residues 476–524 of HRSV F protein connected by a glycine-rich linker (see *Materials and Methods*) (Fig. 1). CD spectroscopy indicates that recRSV-1 is highly helical (≈70% helix content) and extremely thermostable (the midpoint of thermal denaturation [T_m] ≈90°C in the presence of 4 M guanidine-HCl, pH 7.4); recRSV-1 forms a trimer in PBS buffer as judged by sedimentation equilibrium analysis (X.Z. and P.S.K., unpublished results).

Table 1. X-ray data collection and refinement statistics

Data collection	
Resolution range, Å	20.0–2.20
Observed reflections	119,905
Unique reflections	56,973
Completeness, %	91.2 (64.7)*
R_{merge}†	0.041 (0.269)*
Refinement	
Resolution range, Å	10.0–2.30
Protein nonhydrogen atoms	8073
Water molecules	888
R_{cryst}‡	0.233
R_{free}‡	0.286
rms difference from ideal geometry	
Bond lengths, Å	0.008
Bond angles, °	1.2
Average B-factor, Å^2	45.4

*Values in parentheses correspond to highest resolution shell 2.28 to 2.20 Å.

†$R_{merge} = \Sigma\Sigma_j \mid I_j (hkl) - \langle I(hkl)\rangle \mid / \Sigma\Sigma_j \mid \langle I(hkl)\rangle \mid$, where I_j is the intensity measurement for reflection hkl and ⟨I⟩ is the mean intensity over j reflections.

‡R_{cryst} (R_{free}) = $\Sigma \mid |F_{obs}(hkl)| - |F_{calc}(hkl)| \mid / \Sigma \mid F_{obs}(hkl) \mid$, where F_{obs} and F_{calc} are observed and calculated structure factors, respectively. No σ-cutoff was applied. 10% of the reflections were excluded from refinement and used to calculate R_{free}.

Proteolysis of the recRSV-1 protein reveals a protease-resistant core containing the entire HR-N and HR-C regions predicted by LEARNCOIL-VMF. Digestion of recRSV-1 by trypsin generates two major fragments readily separated by reverse-phase HPLC. Mass spectrometry analysis unambiguously assigns these as an N-terminal fragment corresponding to residues 153–209, denoted HRSV-N57 [observed molecular weight (MW) = expected MW = 6,130], and a C-terminal fragment corresponding to residues 476–520, denoted HRSV-C45 (observed MW = expected MW = 5,111) (Fig. 1).

The isolated HRSV-N57 peptide folds into an α-helical structure in PBS (>40% helix content) as determined by CD but does not form a monodisperse species according to sedimentation equilibrium analysis (X.Z. and P.S.K., unpublished results). The apparent T_m of HRSV-N57 varies (≈40–50°C at 10 μM in PBS), presumably due to aggregation. In contrast, the isolated HRSV-C45 peptide is unfolded, and the CD signal does not show a thermal unfolding transition (X.Z. and P.S.K., unpublished results). The CD spectrum of an equimolar mixture of the HRSV-N57 and HRSV-C45 peptides shows a substantially higher α-helical signal than the weighted average of the spectra of the individual peptides, indicating a major conformational change upon association of the two peptides (Fig. 3*A*). The HRSV-N57/C45 complex has an apparent T_m of 88°C at 10 μM in PBS (X.Z. and P.S.K., unpublished results). Sedimentation equilibrium centrifugation clearly indicates that in the HRSV-N57/C45 complex the peptides are present in a 3:3 ratio (Fig. 3*B*). These results are in agreement with those of Lambert and colleagues (28).

HRSV-N57/C45 can be further trimmed by proteinase K to generate smaller fragments denoted HRSV-N51 (residues 157–207) and HRSV-C39 (residues 482–520) (Fig. 1). Proteinase K is not sequence specific; therefore, its proteolytic fragments are expected to better represent the boundaries of a well-folded domain. The HRSV-N51/C39 complex has an apparent T_m of 88°C at 10 μM in PBS (X.Z. and P.S.K., unpublished results), the same as that of HRSV-N57/C45. Thus, the extra-terminal

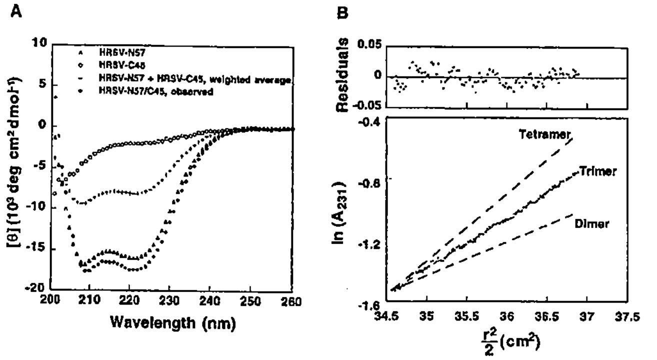

Fig. 3. Biophysical characterization of HRSV peptides. (*A*) CD spectra of HRSV-N57, HRSV-C45, and HRSV-N57/C45 in PBS at 25°C. The predicted spectrum for noninteracting HRSV-N57 plus HRSV-C45 peptides is shown for comparison. (*B*) Equilibrium sedimentation of HRSV-N57/C45 at 20°C and 15,000 rpm in PBS. The data fit closely to a trimeric model. Lines expected for dimeric and tetrameric models are indicated for comparison. The deviation in the data from the linear fit for a trimeric model is plotted (*Upper*). No systematic deviation in the residuals is observed.

residues in HRSV-N57 and HRSV-C45 do not seem to contribute to the stability of the core complex.

Crystal Structure of HRSV-N57/C45. Crystals of HRSV-N57/C45 contain four trimers of HRSV-N57/C45 heterodimers per unit cell, giving rise to 12 independently refined heterodimers. Both the final $2F_o$–F_c map and simulated annealing omit map are readily interpretable (Fig. 4*A*). However, some terminal residues, including 153–159, 208–209, 476–479, and 517–520, are disordered to a different degree among different chains. Although it is possible that this variation is due to the differences in local lattice contact environments, these terminal residues are more likely to be intrinsically flexible, especially in solution, as they are removed in the proteinase K-digested HRSV-N57/C45.

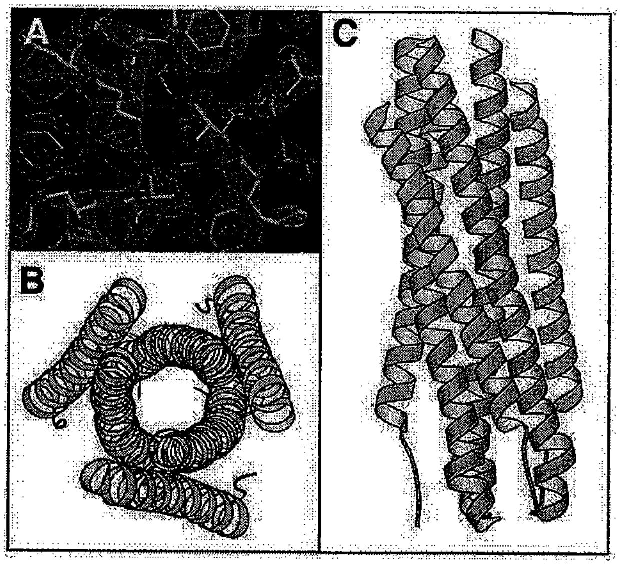

Fig. 4. Crystal structure of HRSV-N57/C45 complex. (*A*) A region of a simulated annealing omit map of HRSV-N57/C45, calculated with $2F_o$–F_c coefficients in the absence of the fragments shown. The map is displayed as a map cover contoured at 1σ. The view is down the 3-fold axis of the trimer. Figure was generated with the program O (36). (*B* and *C*) Ribbon diagram of the HRSV-N57/C45 trimer. N helices are shown in blue and C helices in yellow. (*B*) A top view of the HRSV-N57/C45 trimer looking down the 3-fold axis of the trimer. (*C*) A side view with the amino termini of the N helices pointing toward the top of the page and those of the C helices pointing toward the bottom. Figure was prepared with MOLSCRIPT (45).

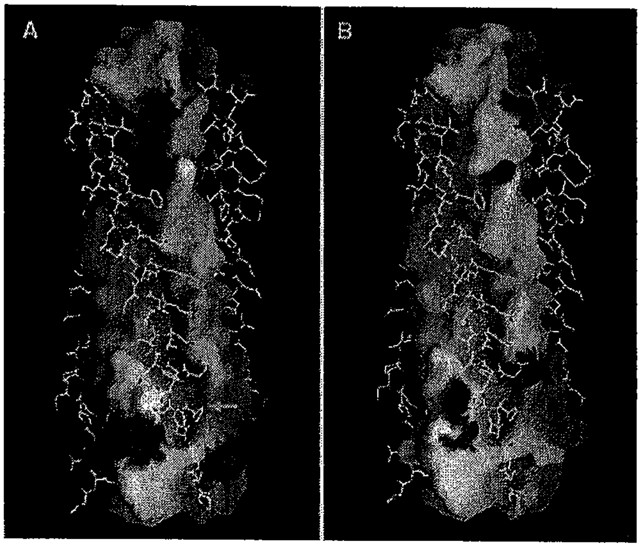

Fig. 5. The surface properties of the HRSV-N57 trimer with the HRSV-C45 peptides displayed in a stick-style representation. View same as Fig. 4C. (*A*) Surface variability of the HRSV-N57 trimer (analysis based on RSV sequences available in GenBank and Swiss-Prot). The residues shown in dark red vary among different human virus strains. The residues shown in pink are identical among 20 human strains of HRSV but are different in bovine respiratory syncytial virus. The cavity region is indicated by a yellow arrow. (*B*) Surface mapping of groups with the potential to form electrostatic and polar interactions. Nitrogen and oxygen atoms from charged amino acid side chains are shown in blue and red, respectively. Nitrogen and oxygen atoms from polar amino acid side chains are shown in yellow. Figure was drawn with the program GRASP (46).

We focused our structural analysis on the well-defined regions, including residues 160–207 in HRSV-N57 and residues 480–516 in HRSV-C45. For these regions, the structural differences between the 12 copies of the HRSV-N57/C45 heterodimer are small (e.g., the average rms difference in C_α positions between any pair of heterodimers is 0.34 Å).

HRSV-N57/C45 forms a rod-shaped, six-helix bundle of approximately 68 Å in length and 27 Å in diameter (Fig. 4 *B* and *C*). The HRSV-N57 peptides form a three-stranded coiled coil. Three HRSV-C45 peptides pack in an antiparallel manner against long, hydrophobic grooves formed on the surface of the HRSV-N57 core. This packing arrangement would put the fusion peptide segment, located immediately before HRSV-N57, and transmembrane segment, located immediately after HRSV-C45, in close proximity.

The Interface Between the HRSV-N57 Core and HRSV-C45. Approximately 3,000 $Å^2$ of solvent-accessible surface area are buried at the interface between the HRSV-N57 core and each HRSV-C45 peptide. Twenty amino acid residues from each HRSV-C45 peptide and 26 residues from two adjacent HRSV-N57 peptides contribute to the interface interaction. These residues are highly conserved among different HRSV strains, including 20 HRSV isolates and seven bovine respiratory syncytial virus isolates (analysis based on sequences available in GenBank and Swiss-Prot as of September 2000) (Fig. 5*A*). Most of the amino acid differences between strains are limited to conservative mutations.

Various features of the deep groove on the surface of the HRSV-N57 trimer (Fig. 5*B*) suggest that this groove is a poten-

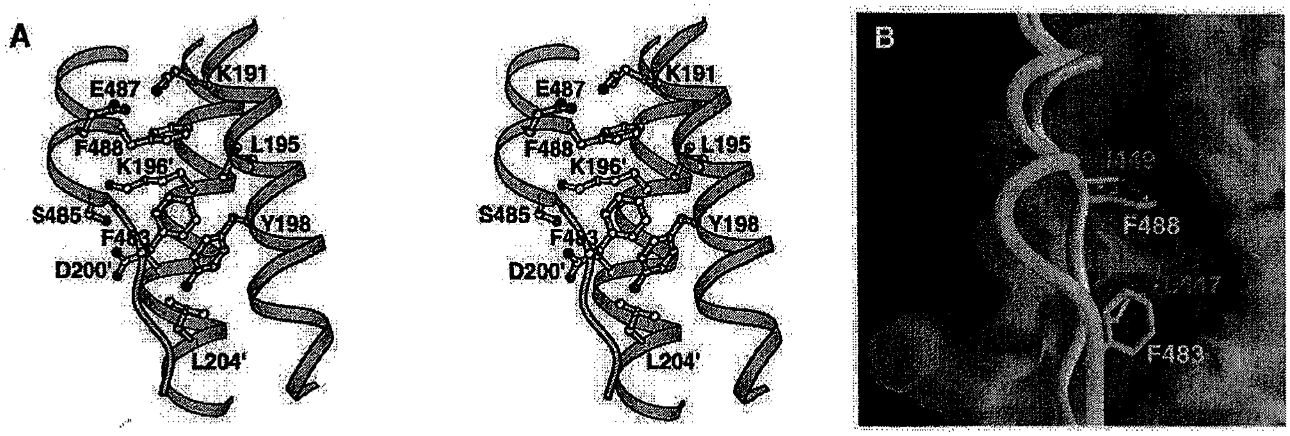

Fig. 6. The cavity on the surface of the HRSV-N57 coiled coil. (*A*) A stereo view of interactions in the HRSV-N57 cavity. Two phenylalanine residues of HRSV-C45 (yellow) fit into the cavity formed by two neighboring HRSV-N57 peptides (blue). A prime symbol is used to distinguish residues from the two HRSV-N57 chains. Figure was prepared with MOLSCRIPT (45). (*B*) Comparison of cavity interactions of the HRSV and SV5 structures. The HRSV-N57 coiled coils, which superimpose closely with the SV5 N peptide coiled coils (21), are represented as a molecular surface (the most convex part shown in green and the most concave in gray). The HRSV-C45 (yellow) and SV5 C peptide (pink) helices are shown as ribbons with selected side chains that pack into the cavity. The relative shift of the C peptides is clearly visible. Figure was drawn with the program GRASP (46).

tially attractive drug target. The carboxyl-terminal end of the groove features a hydrophobic cavity. Within the cavity region, the majority of contacts are between six cavity-lining residues from the HRSV-N57 peptides (Lys-191, Leu-195, and Tyr-198 from one chain and Lys-196, Asp-200, and Leu-204 from another) and two aromatic residues, Phe-483 and Phe-488, from the HRSV-C45 peptide (Fig. 6). A patch in the middle of the hydrophobic groove (Fig. 5*B*) is enriched with polar residues. Multiple hydrogen bonds are observed in this area. For example, Ser-509 Oγ of the HRSV-C45 peptide forms an elaborate hydrogen-bond network with Thr-174 Oγ1, Ala-170 O, and Asn-175 Nδ2 from the HRSV-N57 helices. The abundance of hydrogen-bond donor/acceptors in the groove is likely to greatly enhance binding specificity due to the requirement of electrostatic complementarity. Thus, this cavity and groove are potentially good binding sites for small molecule inhibitors (*cf.* refs. 39–41).

Comparison with SV5 F1 Trimer Core and Other Viral Fusion Proteins. Among paramyxovirus fusion proteins, only the structure of the SV5 F1 trimer core has been determined (21). In general, the F1 core from HRSV and SV5 adopt a similar fold, despite a low sequence identity between the two proteins (18.4% for the entire protein sequence and 19.1% for the HR regions). These structures can be superimposed with an rms difference of 2.1 Å between all C_α atoms. The central N peptide cores superimpose closely, with an rms difference of 0.65 Å, whereas the C peptides are more divergent, with an rms difference of 2.9 Å.

A stutter or increase in spacing pattern (3-4-4-4-3) for HRs, instead of the regular 3-4-3-4-3, has been observed in the SV5 F1 trimer core (21). A similar stutter is observed within the last two HRs in the HRSV-N57 coiled-coil core. This supports the prediction by Baker *et al.* that the 3-4-4-4-3 pattern will be conserved among paramyxovirus F proteins because it can maintain hydrophobic residues within the coiled-coil core (21). However, because the stutter in HRSV-N57 occurs at the end of the peptide helix, structural irregularities resulting from helix end effects cannot be ruled out.

It has been suggested that the C peptides of HRSV and other paramyxoviruses will have a similar main-chain conformation as observed in the SV5 crystal structure (21). However, our results show that the HRSV C peptide has one additional helical turn not observed in the SV5 C peptide. As a consequence, the position of the C peptide residues that pack into the hydrophobic cavity is shifted in HRSV compared with SV5 (Fig. 6*B*), and such a packing arrangement is not readily predicted from primary sequence alignment of the two proteins.

Discussion

The structure of HRSV-N57/C45 adds to the repertoire of viral fusion proteins that have been shown to form a trimer-of-hairpins motif. The remarkable similarity between the HRSV F1 and HIV-1 gp41 core structures, as well as similar C peptide inhibition phenomena, suggest a conserved mechanism of fusion. Similar to HIV-1 gp41, HRSV F1 likely undergoes a series of conformational changes to become fusion active. The distinct conformational states proposed for HIV-1 gp41 (24), including the native state, the prehairpin intermediate, and fusion-active hairpin state, also may apply to HRSV F1. Electron microscopy studies of the full-length F protein reveal two distinct conformations, one cone-shaped and the other lollipop-shaped, which may represent the native and fusion-active states, respectively (42). The HRSV-N57/C45 structure presented here likely corresponds to the fusion-active hairpin conformation, as the hairpin formation is structurally coupled to the apposition of viral and cellular membranes.

The existence of the prehairpin intermediate conformation for the HRSV F protein is strongly supported by the observation that peptides corresponding to the HRSV HR-C regions can efficiently inhibit viral fusion (26). Presumably, these HR-C peptides function by binding to the exposed HR-N regions, thereby blocking the conformational transition to the fusion-active form.

If small, oral, bioavailable molecules that disrupt hairpin formation are identified, they may be effective drugs against viral infection. In the case of HIV-1, a strategy to block hairpin formation has been developed to find D peptide inhibitors of viral entry that bind to a hydrophobic pocket on the surface of the central coiled coil consisting of HIV-1 gp41 N peptides (39). The cavity and well-defined groove on the surface of the central coiled coil of the HRSV-N57/C45 complex identified here may serve as useful drug targets.

Finally, the HRSV-N57/C45 structure may provide a new direction in vaccine development against HRSV infection. Antibodies from vaccine trials using purified, native, full-length F protein have very low neutralizing activities compared with those generated by live HRSV (1). One suggested strategy for eliciting neutralizing HIV-1 antibodies is to target transient intermediates or fusion-competent conformations (39, 43). The N-terminal coiled coil observed in the current structure might be formed in a prehairpin intermediate analogous to that found in HIV-1 and thus may be a viable target for antifusion antibodies. A neutralizing antibody against HRSV has been mapped to the N-terminal coiled-coil region (44); it will be interesting to see whether it targets a prehairpin intermediate.

We thank James Pang for mass spectrometric analysis; Alexandra Evindar and Leslie Gaffney for assistance in preparation of the manuscript and figures; Christopher Liu for valuable comments on the manuscript; Michael Burgess, David Akey, and Brian Schneider for technical assistance and advice; and members of the Kim lab for helpful discussions. We also thank Dr. Craig Ogata and the staff of the Howard Hughes Medical Institute beamline (X4A) at Brookhaven National Laboratory for help in data collection. X.Z. was supported by a postdoctoral fellowship from the Anna Fuller Fund. This work was supported by National Institutes of Health Grants GM44162 and GM56552 and used the W.M. Keck Foundation x-ray Crystallography Facility at the Whitehead Institute.

1. Collins, P. L., McIntosh, K. & Chanock, R. M. (1996) in *Fields Virology*, eds. Fields, B. N., Knipe, D. M. & Howley, P. M. (Lippincott, Philadelphia), pp. 1313–1351.
2. Heilman, C. A. (1990) *J. Infect. Dis.* **161**, 402–406.
3. Johnson, P. R., Spriggs, M. K., Olmsted, R. A. & Collins, P. L. (1987) *Proc. Natl. Acad. Sci. USA* **84**, 5625–5629.
4. Bukreyev, A., Whitehead, S. S., Murphy, B. R. & Collins, P. L. (1997) *J. Virol.* **71**, 8973–8982.
5. Chambers, P., Pringle, C. R. & Easton, A. J. (1990) *J. Gen. Virol.* **71**, 3075–3080.
6. Buckland, R. & Wild, F. (1989) *Nature (London)* **338**, 547.
7. Singh, M., Berger, B. & Kim, P. S. (1999) *J. Mol. Biol.* **290**, 1031–1041.
8. Lamb, R. A. (1993) *Virology* **197**, 1–11.
9. Bullough, P. A., Hughson, F. M., Treharne, A. C., Ruigrok, R. W., Skehel, J. J. & Wiley, D. C. (1994) *J. Mol. Biol.* **236**, 1262–1265.
10. Chen, J., Skehel, J. J. & Wiley, D. C. (1999) *Proc. Natl. Acad. Sci. USA* **96**, 8967–8972.
11. Fass, D., Harrison, S. C. & Kim, P. S. (1996) *Nat. Struct. Biol.* **3**, 465–469.
12. Chan, D. C., Fass, D., Berger, J. M. & Kim, P. S. (1997) *Cell* **89**, 263–273.
13. Weissenhorn, W., Dessen, A., Harrison, S. C., Skehel, J. J. & Wiley, D. C. (1997) *Nature (London)* **387**, 426–430.
14. Tan, K., Liu, J., Wang, J.-H., Shen, S. & Lu, M. (1997) *Proc. Natl. Acad. Sci. USA* **94**, 12303–12308.
15. Malashkevich, V. N., Chan, D. C., Chutkowski, C. T. & Kim, P. S. (1998) *Proc. Natl. Acad. Sci. USA* **95**, 9134–9139.
16. Caffrey, M., Cai, M., Kaufman, J., Stahl, S. J., Wingfield, P. T., Covell, D. G., Gronenborn, A. M. & Clore, G. M. (1998) *EMBO J.* **17**, 4572–4584.
17. Yang, Z. N., Mueser, T. C., Kaufman, J., Stahl, S. J., Wingfield, P. T. & Hyde, C. C. (1999) *J. Struct. Biol.* **126**, 131–144.
18. Malashkevich, V. N., Schneider, B. J., McNally, M. L., Milhollen, M. A., Pang, J. X. & Kim, P. S. (1999) *Proc. Natl. Acad. Sci. USA* **96**, 2662–2667.
19. Weissenhorn, W., Carfi, A., Lee, K. H., Skehel, J. J. & Wiley, D. C. (1998) *Mol. Cell* **2**, 605–616.
20. Kobe, B., Center, R. J., Kemp, B. E. & Poumbourios, P. (1999) *Proc. Natl. Acad. Sci. USA* **96**, 4319–4324.
21. Baker, K. A., Dutch, R. E., Lamb, R. A. & Jardetzky, T. S. (1999) *Mol. Cell* **3**, 309–319.
22. Hughson, F. M. (1997) *Curr. Biol.* **7**, R565–R569.
23. Hernandez, L. D., Hoffman, L. R., Wolfsberg, T. G. & White, J. M. (1996) *Annu. Rev. Cell Dev. Biol.* **12**, 627–661.
24. Chan, D. C. & Kim, P. S. (1998) *Cell* **93**, 681–684.
25. Kilby, J. M., Hopkins, S., Venetta, T. M., DiMassimo, B., Cloud, G. A., Lee, J. Y., Alldredge, L., Hunter, E., Lambert, D., Bolognesi, D., *et al.* (1998) *Nat. Med.* **4**, 1302–1307.
26. Lambert, D. M., Barney, S., Lambert, A. L., Guthrie, K., Medinas, R., Davis, D. E., Bucy, T., Erickson, J., Merutka, G. & Petteway, S. R., Jr. *(1996) Proc. Natl. Acad. Sci. USA* **93**, 2186–2191.
27. Matthews, J. M., Young, T. F., Tucker, S. P. & Mackay, J. P. (2000) *J. Virol.* **74**, 5911–5920.
28. Lawless-Delmedico, M. K., Sista, P., Sen, R., Moore, N. C., Antczak, J. B., White, J. M., Greene, R. J., Leanza, K. C., Matthews, T. J. & Lambert, D. M. (2000) *Biochemistry* **39**, 11684–11695.
29. Makrides, S. C. (1996) *Microbiol. Rev.* **60**, 512–538.
30. Fass, D. & Kim, P. S. (1995) *Curr. Biol.* **5**, 1377–1383.
31. Edelhoch, H. (1967) *Biochemistry* **6**, 1948–1954.
32. Laue, T. M., Shah, B. D., Ridgeway, T. M. & Pelletier, S. L. (1992) in *Analytical Ultracentrifugation in Biochemistry and Polymer Science*, eds. Harding, S. E., Rowe, A. J. & Horton, J. C. (Royal Society of Chemistry, Cambridge), pp. 90–125.
33. Otwinowski, Z. (1993) in *Data Collection and Processing*, eds. Sawer, L., Isaacs, N. & Bailey, S. (SERC, Daresbury Laboratory, Warrington, U.K.), pp. 55–62.
34. CCP4 (1994) *Acta. Crystallogr. D* **50**, 760–763.
35. Kowtan, K. (1994) *Proteins* **31**, 34–38.
36. Jones, T. A., Zou, J. W., Cowan, S. & Kjeldgaard, M. (1991) *Acta Crystallogr. D* **47**, 110–119.
37. Brünger, A. T., Adams, P. D., Clore, G. M., DeLano, W. L., Gros, P., Grosse-Kunstleve, R. W., Jiang, J.-S., Kuszewski, J., Nilges, M., Pannu, N. S., *et al.* (1998) *Acta. Crystallogr. D* **54**, 905–921.
38. Laskowski, R. A., MacArthur, M. W., Moss, D. S. & Thornton, J. M. (1993) *J. Appl. Crystallogr.* **26**, 283–291.
39. Eckert, D. M., Malashkevich, V. N., Hong, L. H., Carr, P. A. & Kim, P. S. (1999) *Cell* **99**, 103–115.
40. Chan, D. C., Chutkowski, C. T. & Kim, P. S. (1998) *Proc. Natl. Acad. Sci. USA* **95**, 15613–15617.
41. Ferrer, M., Kapoor, T. M., Strassmaier, T., Weissenhorn, W., Skehel, J. J., Oprian, D., Schreiber, S. L., Wiley, D. C. & Harrison, S. C. (1999) *Nat. Struct. Biol.* **6**, 953–960.
42. Calder, L. J., Gonzalez-Reyes, L., Garcia-Barreno, B., Wharton, S. A., Skehel, J. J., Wiley, D. C. & Melero, J. A. (2000) *Virology* **271**, 122–131.
43. LaCasse, R. A., Follis, K. E., Trahey, M., Scarborough, J. D., Littman, D. R. & Nunberg, J. H. (1999) *Science* **283**, 357–362.
44. Langedijk, J. P., Meloen, R. H. & van Oirschot, J. T. (1998) *Arch. Virol.* **143**, 313–320.
45. Kraulis, P. J. (1991) *J. Appl. Crystallogr.* **24**, 946–950.
46. Nicholls, A., Sharp, K. A. & Honig, B. (1991) *Proteins* **11**, 281–296.
47. Navaza, J. (1994) *Acta. Crystallogr. A* **50**, 157–163.

NCBI PubMed www.pubmed.gov

A service of the National Library of Medicine
and the National Institutes of Health

My NCBI
[Sign In] [Regis

All Databases PubMed Nucleotide Protein Genome Structure OMIM PMC Journals Boo

Search PubMed for Go Clear

Limits Preview/Index History Clipboard Details

Display AbstractPlus Show 20 Sort By Send to

All: 1 Review: 0

1: Virology. 1998 Aug 15;248(1):20-34.

ELSEVIER FULL-TEXT ARTICLE Links

A core trimer of the paramyxovirus fusion protein: parallels to influenza virus hemagglutinin and HIV-1 gp41.

Joshi SB, **Dutch RE**, **Lamb RA**.

Department of Biochemistry, Molecular Biology and Cell Biology, Northwestern University, Evanston, Illinois, 60208-3500, USA.

The paramyxovirus fusion (F) protein mediates membrane fusion. The biologically active F protein consists of a membrane distal subunit, F2, and a membrane-anchored subunit, F1. We have identified a highly stable structure composed of peptides derived from the F1 heptad repeat A, which abuts the hydrophobic fusion peptide (peptide N-1), and the F1 heptad repeat B, located 270 residues downstream and adjacent to the transmembrane domain (peptides C-1 and C-2). In isolation, peptide N-1 is 47% alpha-helical and peptide C-1 and C-2 are unfolded. When mixed together, peptides N1 + C1 form a thermostable (Tm >90 degreesC), 82% alpha-helical, discrete trimer of heterodimers (mass 31,300 Mr) that is resistant to denaturation by 2% SDS at 40 degreesC. We suggest that this alpha-helical trimeric complex represents the core most stable form of the F protein that either is fusion competent or forms after fusion has occurred. Peptide C-1 is a potent inhibitor of both the lipid mixing and the aqueous content mixing fusion activity of the SV5 F protein. In contrast, peptides N-1 and N-2 inhibit cytoplasmic content mixing but not lipid mixing, leading to a stable hemifusion state. Thus, these peptides define functionally different steps in the fusion process. The parallels among both the fusion processes and the protein structures of paramyxovirus F proteins, HIV gp41, and influenza virus hemagglutinin are discussed, as the analogies are indicative of a conserved paradigm for fusion promotion among fusion proteins from widely disparate viruses. Copyright 1998 Academic Press.

PMID: 9705252 [PubMed - indexed for MEDLINE]

Related Links

The paramyxovirus fusion protein forms an extremely stable core trimer: structural parallels to influenza virus haemagglutinin an[Mol Membr Biol. 1999]

Paramyxovirus fusion protein: characterization of the core trimer, a rod-shaped complex with helices in anti-parallel orientation. [Virology. 1999]

Crystal structure of the simian immunodeficiency virus (SIV) gp41 core: conserved helical interactions underlie the broad inhibitory activity of gp41 peptid[Proc Natl Acad Sci U S A. 1998]

Core structure of gp41 from the HIV envelope glycoprotein. [Cell. 1997]

Secondary structure, orientation, oligomerization, and lipid interactions of the transmembrane domain of influenza hemaggluti[Biochemistry. 2000]

See all Related Articles...

Display AbstractPlus Show 20 Sort By Send to

Write to the Help Desk
NCBI | NLM | NIH

Department of Health & Human Services
Privacy Statement | Freedom of Information Act | Disclaimer

NCBI PubMed www.pubmed.gov

A service of the National Library of Medicine and the National Institutes of Health

My NCBI
[Sign In] [Regis

All Databases PubMed Nucleotide Protein Genome Structure OMIM PMC Journals Bool

Search PubMed for Go Clear

Limits Preview/Index History Clipboard Details

Display AbstractPlus Show 20 Sort By Send to

All: 1 Review: 0

☐ **1:** Mol Cell. 1999 Mar;3(3):309-19.

Cell Press Links

Structural basis for paramyxovirus-mediated membrane fusion.

Baker KA, **Dutch RE**, **Lamb RA**, **Jardetzky TS**.

Department of Biochemistry, Molecular Biology, and Cell Biology, Northwestern University, Evanston, Illinois 60208-3500, USA.

Paramyxoviruses are responsible for significant human mortality and disease worldwide, but the molecular mechanisms underlying their entry into host cells remain poorly understood. We have solved the crystal structure of a fragment of the simian parainfluenza virus 5 fusion protein (SV5 F), revealing a 96 A long coiled coil surrounded by three antiparallel helices. This structure places the fusion and transmembrane anchor of SV5 F in close proximity with a large intervening domain at the opposite end of the coiled coil. Six amino acids, potentially part of the fusion peptide, form a segment of the central coiled coil, suggesting that this structure extends into the membrane. Deletion mutants of SV5 F indicate that putative flexible tethers between the coiled coil and the viral membrane are dispensable for fusion. The lack of flexible tethers may couple a final conformational change in the F protein directly to the fusion of two bilayers.

PMID: 10198633 [PubMed - indexed for MEDLINE]

Related Links

Structural basis for coronavirus-mediated membrane fusion. Crystal structure of mouse hepatitis virus spike protein fusion co[J Biol Chem. 2004]

A dual-functional paramyxovirus F protein regulatory switch segment: activation and membrane [J Cell Biol. 2003]

Proper spacing between heptad repeat B and the transmembrane domain boundary of the paramyxovirus SV5 F protein is critical for biol[Virology. 1997]

Sendai virus internal fusion peptide: structural and functional characterization and a plausible mode of viral entry inhibiti[Biochemistry. 2000]

Paramyxovirus F1 protein has two fusion peptides: implications for the mechanism of membrane [J Mol Biol. 2000]

See all Related Articles...

Display AbstractPlus Show 20 Sort By Send to

Write to the Help Desk
NCBI | NLM | NIH
Department of Health & Human Services
Privacy Statement | Freedom of Information Act | Disclaimer

1: Virology. 2001 Oct 25;289(2):343-52. ELSEVIER FULL-TEXT ARTICLE Links

Mutational analysis of the membrane proximal heptad repeat of the newcastle disease virus fusion protein.

McGinnes LW, Sergel T, Chen H, Hamo L, Schwertz S, Li D, Morrison TG.

Department of Molecular Genetics and Microbiology, University of Massachusetts Medical School, 55 Lake Avenue North, Worcester, Massachusetts 01532, USA.

Paramyxovirus fusion proteins have two heptad repeat domains, HR1 and HR2, that have been implicated in the fusion activity of the protein. Peptides from these two domains form a six-stranded, coiled-coil with the HR1 sequences forming a central trimer and three molecules of the HR2 helix located within the grooves in the central trimer (Baker et al., 1999, Mol. Cell 3, 309; Zhao et al. 2000, Proc. Natl. Acad. Sci. USA 97, 14172). Nonconservative mutations were made in the HR2 domain of the Newcastle disease virus fusion protein in residues that are likely to form contacts with the HR1 core trimer. These residues form the hydrophobic face of the helix and adjacent residues ("a" and "g" positions in the HR2 helical wheel structure). Mutant proteins were characterized for effects on synthesis, steady-state levels, proteolytic cleavage, and surface expression as well as fusion activity as measured by syncytia formation, content mixing, and lipid mixing. While all mutant proteins were transport competent and proteolytically cleaved, these mutations did variously affect fusion activity of the protein. Nonconservative mutations in the "g" position had no effect on fusion. In contrast, single changes in the middle "a" position of HR2 inhibited lipid mixing, content mixing, and syncytia formation. A single mutation in the more carboxyl-terminal "a" position had minimal effects on lipid mixing but did inhibit content mixing and syncytia formation. These results are consistent with the idea that the HR2 domain is involved in posttranslational interactions with HR1 that mediate the close approach of membranes. These results also suggest that the HR2 domain, particularly the carboxyl-terminal region, plays an additional role in fusion, a role related to content mixing and syncytia formation. Copyright 2001 Academic Press.

PMID: 11689056 [PubMed - indexed for MEDLINE]

enzyme to free the virus from the cell surface. The receptor for CDV and other morbilliviruses is not yet known.

The structure of the Pneumovirus attachment protein (G) is very different from the attachment protein of the *Paramyxovirinae*. The RSV G protein has neither hemagglutinating nor neuraminidase activity. The nucleotide sequence of the RSV G gene predicts that the protein is of about 289 to 299 amino acids (M_r 32,587), and it is a type II integral membrane protein with a single N-terminal hydrophobic signal/anchor domain (247,289). The G protein is found in virus-infected cells in both membrane-bound and proteolytically cleaved soluble forms. The distinguishing feature of the RSV G protein is the extent of its carbohydrate modification. On SDS polyacrylamide gel electrophoresis, the protein migrates with an apparent M_r of about 84,000 to 90,000, and the dramatic increase in molecular weight over that predicted for the polypeptide chain is because 8 to 12 kd is caused by the addition of N-linked carbohydrate (four potential addition sites) and 40 to 50 kd is caused by the addition of O-linked glycosylation (77 potential acceptor serine or threonine residues; 30% of total residues) (44,290, and references therein). Quite remarkably, it appears the RSV G protein is not essential for virus assembly or growth in tissue culture or animals, but it does confer a growth advantage. A virus that had been extensively passaged in cells was found to contain a spontaneous deletion of the G and SH genes (146), yet the virus replicated in Vero cells. In addition, the G gene has been deleted from recombinant virus recovered from an infectious cDNA clone (see Chapter 45). These finding suggest that RSV has an alternative mechanism for attachment to cells that does not involve G protein.

Fusion Protein

The Paramyxovirus fusion (F) proteins mediate viral penetration by fusion between the virion envelope and the host cell plasma membrane, and this fusion event occurs at neutral pH. The consequence of the fusion reaction is that the nucleocapsid is delivered to the cytoplasm. Later in infection, the F proteins expressed at the plasma membrane of infected cells can mediate fusion with neighboring cells to form syncytia (giant cell formation), a cytopathic effect that can lead to tissue necrosis *in vivo* and might also be a mechanism of virus spread.

Paramyxovirus fusion proteins are synthesized as an inactive precursor (F_0) that is cleaved by a host-cell protease. This releases the new N-terminus of F_1, thus forming the biologically active protein consisting of the disulfide-linked chains F_1 and F_2 (128,250). The Paramyxovirus F genes encode 540 to 580 residues (see Fig. 13). The F proteins are type I integral membrane proteins, which span the membrane once and contain at their N-terminus a cleavable signal sequence that targets the nascent polypeptide chain synthesis to the membrane of the ER. At their C-termini, a hydrophobic stop-transfer domain (a TM domain) anchors the protein in the membrane, leaving a short cytoplasmic tail (about 20 to 40 residues). Comparison of the amino acid sequences of Paramyxovirus F proteins (reviewed in ref. 192) does not show overall major regions of sequence identity, but the similar placement of cysteine, glycine, and proline residues together with the overall hydrophobicity of the F proteins suggests a similar structure for all F proteins. The Respirovirus and Rubulavirus F_2 and F_1 subunits are glycosylated and there are a total of three to six potential sites for the addition of N-linked carbohydrate. For SV5 F protein, it is known that all four potential sites for addition of N-linked carbohydrate are used (7). The Morbillivirus F protein contains three sites in the F_2 subunit for N-linked carbohydrate addition, and all three sites are used, and there are no sites in F_1 for N-linked carbohydrate addition (2).

Protein sequencing studies of the F protein and nucleotide sequencing studies of the F genes have indicated that the N-terminal 25 residues of F_1 (fusion peptide) are extensively hydrophobic and this region of the F protein is highly conserved among F proteins of the *Paramyxovirinae* (up to 90% identity) (Fig. 15). The Paramyxovirus fusion peptides are thought to intercalate into target membranes, initiating the fusion process, and evidence for direct insertion into bilayers has been obtained using hydrophobic photoaffinity labeling probes (204). It has also been shown that the fusion peptides are sufficiently hydrophobic that they can act as a TM anchor domain to convert a formerly soluble protein to a membrane-bound form (210). The invariant nature of many of the residues of the fusion peptide between Paramyxovirus F proteins suggests a role more complex than preservation of hydrophobic residues required for a membrane-intercalating domain; neither signal sequences nor membrane anchorage domains show sequence conservation beyond their hydrophobic nature. It has been noted that if the fusion peptide is assumed to be an α-helix, then the invariant residues are located on one face of the helix (255). Interestingly, in a study on the conserved residues of the fusion peptide when the glycine residues at position 3, 7, or 12 were changed to alanine, and the altered F proteins expressed, a dramatic increase in syncytium formation was observed (130). Thus, the invariant amino acids in the fusion peptide may preserve a balance between high fusion activity and successful viral replication, as high fusion activity is deleterious to cell viability.

The fusion proteins of several widely disparate viruses share several important common features. The Paramyxovirus F protein, the human and simian immunodeficiency virus (HIV and SIV) gp160, Ebola virus GP, and influenza virus hemagglutinin (HA) protein all form homotrimers (26,39,85,237,296) that must be proteolytically cleaved to be biologically active (144,153,250). The resulting TM domain–containing subunits (Paramy

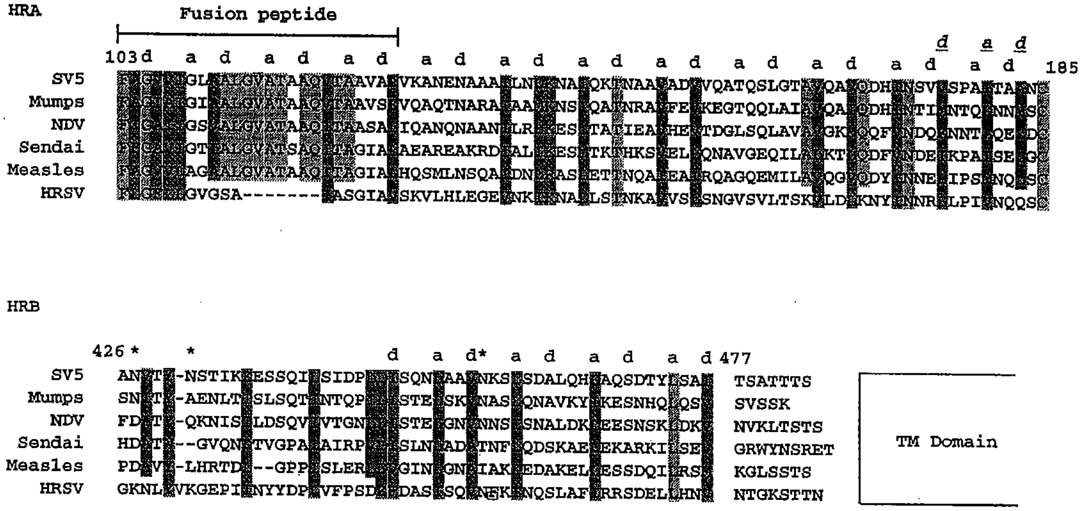

FIG. 15. Sequence alignment of the fusion peptide and the heptad repeats HRA and HRB of the SV5 F protein with that of other paramyxoviruses. Conserved residues among members of the *Paramyxovirinae* (i.e., not including hRSV) are *shaded light gray* and residues with similar properties (hydrophobic or charged) are *shaded dark gray*. Those residues that are also conserved in HRSV, which is evolutionarily distant from other paramyxoviruses, are indicated in the HRSV sequence with the appropriate shading. Letters immediately above the sequence indicate the predicted hydrophobic heptad repeat a and *d* residues. The predicted heptad is incorrect for residues 175 to 184, and the observed *a* and *d* residues in the atomic structure (see Fig. 16) are indicated above the predicted repeat and underlined. *Asterisks* indicate N-linked carbohydrate sites for the SV5 F protein. The SV5 sequence is numbered. NDV, Newcastle disease virus; HRSV, human respiratory syncytial virus. (Adapted from ref. 8, with permission.).

ovirus F, F_1; HIV gp160, gp41; Ebola GP, GP2; influenza HA, HA_2), contain a hydrophobic fusion peptide at the new N-termini, which has been shown to insert into the target membrane during the fusion process (4,65,104, 118). Additionally, two 4-3 heptad repeat regions are present in each of these fusion proteins, one near the fusion peptide and one in close proximity to the TM domain (20,38). These regions are thought to be important in the fusion reaction, as mutations within these domains frequently lead to a fusion-deficient phenotype (29,42,240, 254), and peptides corresponding to these regions have been demonstrated to block the fusion process (139,142, 165,177,196,229,293,294,297,300).

The atomic structure of uncleaved and cleaved influenza virus HA are known (40,296). However, this is not the case for the intact glycoproteins HIV-1/SIV gp160, Ebola virus GP, or the Paramyxovirus F protein. However, biochemical, EM, nuclear magnetic resonance, and x-ray crystallographic analyses of most of HA_2 (22), portions of HIV-1/SIV gp41 (12,25,39,177,264,286,287), a portion of a retrovirus Env-TM domain (85), and most of Ebola virus GP2 (178,285) indicate that their heptad repeat regions show considerable similarity in that they all form trimeric coiled coils, with the N-terminal heptad repeat forming an interior, trimeric coiled coil surrounded by three antiparallel helices. This structure has been suggested to represent the final, most stable form of the protein, present either during or subsequent to membrane fusion, with peptide inhibitors most likely functioning by preventing formation of this core (12,177).

The Paramyxovirus F protein membrane proximal subunit (F_1) differs from that of HA_2, gp41, Env-TM, and GP2 because its ectodomain is much larger in size (383 residues versus 120 to 185 residues). F_1 contains two heptad repeat regions, one (HRA) adjacent to the fusion peptide and the other (HRB) adjacent to the TM domain (see Fig. 13). In contrast to the HA_2, gp41, Env-TM, and GP2 just described, where heptad repeats are separated only by small spacer regions, in paramyxoviruses about 250 residues separate the heptad repeat regions. Nonetheless, biochemical and EM analysis indicated that the Paramyxovirus heptad repeat peptides form a rod-shaped structure approximately 96 Å in length. Peptides (N-1) derived from HRA form a three-stranded α-helical coiled coil around which three peptides (C-1) derived from HRB are packed in an antiparallel manner. The N-terminus of N-1 and the C-terminus of C-1 are localized to the same end of the rod, placing the fusion peptides and TM domains close together (77,142). These biochemical data were confirmed by solving the crystal structure of the SV5 F_1 N-1/C-1 complex to 1.4 Å resolution (8). The 64 amino acids of N-1 fold into an 18-turn α-helix stretching the entire length of the coiled coil. The C-terminal 25 residues of C-1 form a seven-turn amphipathic α-helix, whereas amino acids 440 to 450 form an extended chain (Figs. 16 and 17).

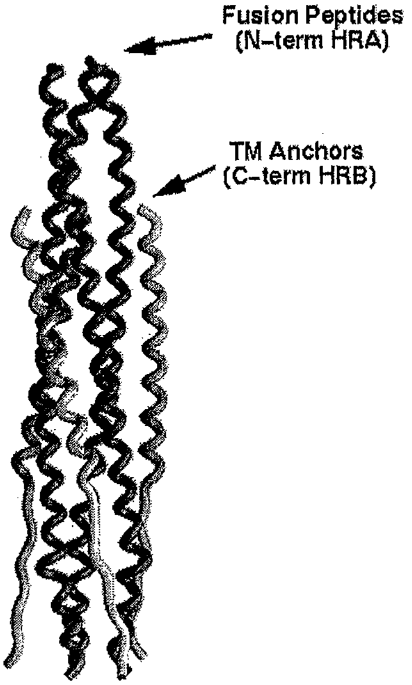

FIG. 16. The SV5 F1 core trimer structure. The complete SV5 F1 core trimer is shown. The central HRA (N-1) trimeric coiled coil is shown in *dark gray* and the buttressing antiparallel HRB (C-1) helices are shown in *light gray.* (Adapted from ref. 8, with permission.)

Despite the similarity of core structure among these viral fusion proteins, there are important differences between the Paramyxovirus F proteins and other viral fusion proteins. Unlike influenza virus HA protein and HIV gp160, the Paramyxovirus F protein does not provide the primary binding role for the virus: Paramyxovirus primary binding to a target cell is mediated by the HN glycoprotein. However, as mentioned before, at least two *Paramyxoviridae* F proteins, those of Sendai and RSVs, appear to have attachment activity.

A large body of evidence suggests that viral fusion proteins undergo a conformational change to become fusion active (reviewed in ref. 117). For influenza virus HA, the cleaved HA (296) exists in a metastable conformation, trapped from achieving its lower-energy fusogenic conformation by a kinetic barrier. During virus uncoating in endosomes, the low pH environment of the endosomal lumen triggers a conformational change in HA, in which two separate α-helical regions in HA_2 (296) rearrange to form a single triple-stranded coiled coil (22,41). After this conformational change, the fusion peptide is relocated by about 100 Å to one end of the rod-shaped coiled coil (22): the basis of the "spring-loaded mechanism" of fusion (30). For HIV-1 gp120/gp41 and retrovirus Env-SU+Env-TM, binding to the viral receptor may induce the conformational change to release the

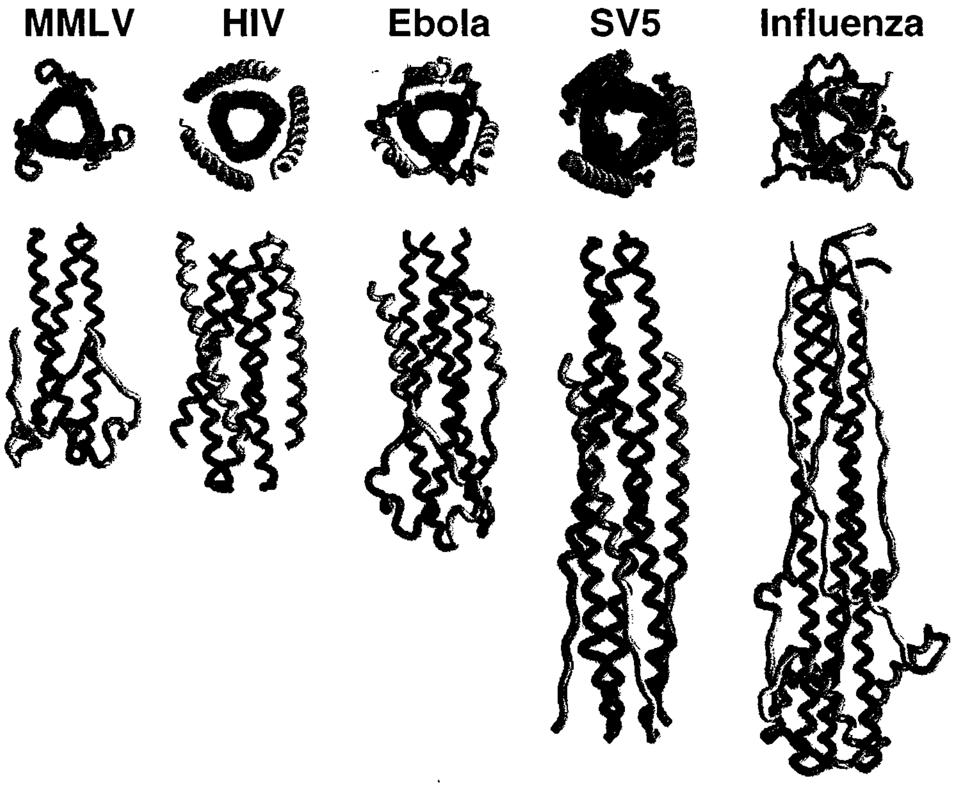

FIG. 17. Comparison of the SV5 F1 core trimer to other viral fusion protein structures. The proteins under comparison include the low-pH-induced influenza virus HA, $tBHA_2$, (22,41), HIV gp41 (39), murine Moloney leukemia virus Env-TM protein (85), and Ebola virus GP2 (285). The interior coiled coil is *dark gray* and the exterior polypeptide is *light gray.* Top and side views are shown for each molecule. (Adapted from ref. 8, with permission.)

fusion peptide (65,91,189). The trigger for the putative conformational changes of Paramyxovirus F proteins is unknown, although as described later for many paramyxoviruses there is a requirement for HN in mediating the fusion reaction (reviewed in ref. 161).

Although the Paramyxovirus F protein is the principal viral glycoprotein involved in virus–cell and cell–cell fusion, the emerging picture indicates the presence of a complex biologic machine. The SV5, measles virus, or RSV F cDNAs when expressed in mammalian cells cause syncytium formation (1,2,131,143,206,209,214), although it is important to note it is likely that many more cells express the F protein than are found in multinucleated cells (209). However, for many other paramyxoviruses including NDV, hPIV-2, hPIV-3, bPIV-3, mumps virus, and CDV (37,78,131,135,191,242,271,295,298) coexpression of F and HN (H for the morbilliviruses) is required for syncytium formation. Furthermore, there is a requirement that the homologous (i.e., of the same virus) HN, and not a heterologous HN, be coexpressed in the same cell (131,135, 253). Thus, it has been suggested that a type-specific interaction occurs between the HN and F protein that is necessary for fusion to occur (135,161,253). A great deal of effort has been spent to map the regions of F and HN that interact. Mutations have been identified in the HN globular domain (68,188), stalk region (253,260,302), and TM anchor (17,185) that decrease or abolish fusogenic activity with no effect on receptor recognition. Analysis of the fusion-promoting activity of chimeric HN molecules derived from different paramyxoviruses suggests that both the TM domain (with much of the stalk region) and parts of the globular head impart F specificity (70,265,278). Coimmunoprecipitation assays also indicate that F and HN can exist in a complex (259,298), and that for hPIV-3, F and HN undergo antibody-induced co-capping indicative of protein complex formation (298). Perhaps most intriguingly, a point mutation was found in the NDV HN globular head that abolishes both its receptor recognition and neuraminidase activity, and that also abolishes its ability to interact with F in coimmunoprecipitation assays (69). These latter data suggest that HN interacts with F only after binding its receptor.

A model that would rationalize the involvement of HN (or H) in fusion promotion is one in which the hypothesized conformational change in F to release the fusion peptide is highly regulated. For those *Paramyxovirinae* that require HN (or H) and F to be coexpressed to observe fusion, the first step would be the binding of HN (or H) to its receptor. On binding ligand, the HN (or H) protein would undergo its own conformational change, which in turn could trigger a conformational change in F to release the fusion peptide. In this way, F and HN operate as a coupled molecular scaffold to release and direct the fusion peptide to the target membrane (reviewed in ref. 161). Examination of mutants of SV5 F protein that require coexpression of HN to mediate fusion indicates that the HN function for F protein triggering can be supplanted by providing energy from raising the temperature, suggesting that the F–HN interaction provides energy to convert cleaved F from a metastable form to a fusogenic form (213).

Cleavage Activation

As discussed, the precursor F_0 molecule is biologically inactive and cleavage of F_0 to the disulfide linked subunits F_1 and F_2 activates the protein, rendering the molecule fusion-active and permitting viral infectivity. Thus, cleavage of F_0 is a candidate to be a key determinant for infectivity and pathogenicity, and for certain viruses this appears to be the case. Proteolytic activation of F_0 involves the sequential action of two enzymes, the host protease that cleaves at the carboxyl side of an arginine residue, and a host carboxypeptidase that removes the basic residues. The *Paramyxoviridae* can be divided into two groups: those that have F proteins with multiple basic residues at the cleavage site and those with F proteins that have a single basic residue at the cleavage site (Table 3). Cleavage of F proteins containing multiple basic residues at the cleavage site occurs intracellularly during transport of the protein through the *trans* Golgi network.

Furin is a cellular protease localized to the *trans* Golgi network, and its sequence specificity for cleavage is R-X-K/R-R. The available evidence suggests that furin, a subtilisin-like endoprotease, is the (or one of the) protease(s) that cleaves F proteins intracellularly (207; reviewed in ref. 153).

Paramyxoviruses that have F proteins with single basic residues in the cleavage site (e.g., Sendai virus) are not usually cleaved when grown in tissue culture and, thus, only a single cycle of growth is obtained. However, the F_0 precursor that is expressed at the cell surface and incorporated into released virions can be cleavage-activated by the addition of exogenous protease (250), leading to multiple rounds of replication.

TABLE 3. *Amino acid sequences upstream of the F protein cleavage site of some members of the* Paramyxoviridae

Sendai virus	G - V - P - Q - S - R ↓
hPIV1	D - N - P - Q - S - R ↓
hPIV3	D - P - **R** - T - **K** - **R** ↓
SV5	T - R - **R** - R - **R** - **R** ↓
Mumps	S - R - **R** - H - **K** - **R** ↓
NDV (virulent strain)	G - R - **R** - Q - $\frac{\mathbf{R}}{\mathbf{K}}$ - **R** ↓
NDV (avirulent strain)	$\frac{G}{E}$ - G - $\frac{K}{R}$ - Q - $\frac{G}{S}$ - R ↓
Measles	S - R - **R** - H - **K** - **R** ↓
RS V	K - K - **R** - K - **R** - **R** ↓

Consensus sequence for furin protease cleavage is

R - X - $\frac{\mathbf{R}}{\mathbf{K}}$ - **R** ↓

Data from Hosaka et al. (125).

Purification of a protease from the allantoic fluid of embryonated chicken eggs has indicated that the endoprotease responsible for Sendai virus activation is homologous to the blood clotting factor Xa, a member of the prothrombin family (100,102). A protease with a similar substrate specificity is secreted from Clara cells of the bronchial epithelium in rats and mice, and this enzyme is probably responsible for activating paramyxoviruses in the respiratory tract. For NDV, the nature of the cleavage site correlates with virulence of the virus. Those strains with multiple basic residues in the F_0 cleavage site are virulent and readily disseminate through the host, whereas those strains with F_0 molecules having single basic residues are avirulent and tend to be restricted to the respiratory tract where the necessary secreted protease can be found (199).

Other Envelope Proteins

The rubulaviruses SV5 and mumps virus both contain a small gene located between F and HN, designated SH (122,123). The SV5 SH protein is a 44-residue, type II integral membrane protein that is expressed at the plasma membrane and is packaged in virions (see Fig. 12). The functional role of SH in the replicative cycle of SV5 is unknown, and in tissue culture cells it can be deleted from an infectious cDNA and recombinant SV5 recovered (111). For mumps virus, although an mRNA transcript derived from the SH gene has been detected (81,82), identification of the SH protein was accomplished only recently (262).

Members of the *Pneumovirinae* also encode an SH protein. The RSV SH protein contains 64 amino acids and is expressed at the plasma membrane of RSV-infected cells as a type II integral membrane protein, and it is packaged in virions (49,205). In RSV-infected cells, four SH-related polypeptide species have been identified: The M_r 4,800 species is thought to result from the initiation of protein synthesis at an internal AUG codon; the M_r 7,500 species is unglycosylated SH; the M_r 13,000 to 15,000 species is SH containing one high mannose N-linked carbohydrate chain; and the M_r 21,000 to 30,000 species is generated by the addition of polylactosaminoglycan to the N-linked carbohydrate chain (3,205). The SH gene was found to be deleted spontaneously from a virus passaged extensively *in vitro* (146), and it has been deleted from recombinant RSV (21) with only minor alterations in virus growth properties in tissue culture cells, or in the respiratory tract of mice or chimpanzees. Thus, the role of the SH protein in the RSV life cycle is not understood.

Pneumovirus M2 Gene

The RSV M2 gene contains two partially overlapping ORFs, designated M2-1 and M2-2, which give rise to two proteins, M2-1 (194 amino acids) and M2-2 (90 amino acids), respectively (47). The mechanism for translating the M2-2 ORF is not clear, but it may involve a ribosomal stop-restart mechanism analogous to that used for synthesis of the influenza B virus BM2 protein (132) (see Chapter 46). The M2-1 protein is an essential transcriptional elongation factor (45,87), and in its absence the polymerase does not transcribe beyond the NS1 and NS2 genes (87). The M2-1 gene also increases RNAP processivity across the gene junctions, attenuating transcriptional termination (87,106,107). The M2-2 gene is not essential for RSV growth, as it can be deleted from a recombinant RSV (11,140). However, the ΔM2-2 virus grows slowly in tissue culture and there is an increase in transcription and decrease in RNA replication (11,140), suggesting that M2-2 protein is involved in regulating transcription and RNA replication.

Pneumovirus NS1 and NS2 Genes

The RSV NS1 (139 amino acids) and NS2 (124 amino acids) are considered to be nonstructural proteins, although the difficulty in purifying virions from contaminating infected-cell debris for this poorly growing virus makes this assignment provisional. Neither protein is thought to be essential for virus growth in cultured cells or in chimpanzees, as the genes can be deleted from a recombinant RSV, but growth *in vitro* and *in vivo* is reduced substantially (19,273,292). In a minireplicon system, when NS1 was expressed, it was inhibitory to both transcription and replication (5), and expression of NS2 at high levels had a small inhibitory effect on transcription and replication (272). Thus, the role of these accessory proteins in the RSV life cycle remains to be fully understood.

STAGES OF REPLICATION

As far as is known, all aspects of the replication of *Paramyxoviridae* take place in the cytoplasm. An overview of the life cycle of the virus is shown schematically in Figure 18, and a diagram indicating the differences between transcription and replication is shown in Figure 19. Unlike in influenza viruses, mRNA synthesis in *Paramyxoviridae* is insensitive to DNA intercalating drugs such as actinomycin D (reviewed in ref. 43), and the *Paramyxoviridae* can replicate in enucleated cells (221). In cell culture, single-cycle growth curves are generally of 14 to 30 hours duration, but they can be as short as 10 hours for virulent strains of NDV. The effect of viral replication on host macromolecular synthesis is quite variable, ranging from almost complete shutoff late in infection for NDV, to no obvious effect with SV5.

FIELDS

VIROLOGY

Fourth Edition

Volume 1

Editors-in-Chief

David M. Knipe, Ph.D.
Higgins Professor of Microbiology
and Molecular Genetics
Harvard Medical School
Boston, Massachusetts

Peter M. Howley, M.D.
George Fabyan Professor of Comparative Pathology
Department of Pathology
Harvard Medical School
Boston, Massachusetts

Associate Editors

Diane E. Griffin, M.D., Ph.D.
Department of Molecular Biology and Immunology
Johns Hopkins School of Public Health
Baltimore, Maryland

Robert A. Lamb, Ph.D., Sc.D.
Howard Hughes Medical Institute
Department of Biochemistry, Molecular Biology,
and Cell Biology
Northwestern University
Evanston, Illinois

Malcolm A. Martin, M.D.
Laboratory of Molecular Microbiology
National Institute of Allergy and Infectious Diseases
National Institutes of Health
Bethesda, Maryland

Bernard Roizman, Sc.D.
Departments of Molecular Genetics and Cell
Biology and Molecular Biology and Biochemistry
University of Chicago
Chicago, Illinois

Stephen E. Straus, M.D.
Chief, Laboratory of Clinical Investigation
National Institute of Allergy and Infectious Diseases
Director, National Center for Complementary and Alternative Medicine
National Institutes of Health
Bethesda, Maryland

LIPPINCOTT WILLIAMS & WILKINS
A **Wolters Kluwer** Company
Philadelphia • Baltimore • New York • London
Buenos Aires • Hong Kong • Sydney • Tokyo

Acquisitions Editor: Jonathan Pine
Developmental Editor: Anne Snyder
Production Editor: Robin E. Cook
Manufacturing Manager: Tim Reynolds
Cover Designer: Patricia Gast
Compositor: Lippincott Williams & Wilkins Desktop Division
Printer: Courier Westford

© 2001 by LIPPINCOTT WILLIAMS & WILKINS
530 Walnut Street
Philadelphia, PA 19106 USA
LWW.com

All rights reserved. This book is protected by copyright. No part of this book may be reproduced in any form or by any means, including photocopying, or utilized by any information storage and retrieval system without written permission from the copyright owner, except for brief quotations embodied in critical articles and reviews. Materials appearing in this book prepared by individuals as part of their official duties as U.S. government employees are not covered by the above-mentioned copyright.

Printed in the USA

Library of Congress Cataloging-in-Publication Data

Fields' virology / editors-in-chief, David M. Knipe, Peter M. Howley ; associate editors,
Diane E. Griffin ... [et al.].—4th ed.
p. ; cm.
Includes bibliographical references and index.
ISBN 0-7817-1832-5
1. Virology. I. Title: Virology. Fields, Bernard N. III. Knipe, David M. (David
Mahan), 1950–IV. Howley, Peter M. V., Griffin, Dianbe E.
[DNLM: 1. Viruses. 2. Virus Diseases. QW 160 F463 2001]
QR360.V5125 2001
616'.0194—dc21

00-067800

Care has been taken to confirm the accuracy of the information presented and to describe generally accepted practices. However, the authors, editors, and publisher are not responsible for errors or omissions or for any consequences from application of the information in this book and make no warranty, expressed or implied, with respect to the currency, completeness, or accuracy of the contents of the publication. Application of this information in a particular situation remains the professional responsibility of the practitioner.

The authors, editors, and publisher have exerted every effort to ensure that drug selection and dosage set forth in this text are in accordance with current recommendations and practice at the time of publication. However, in view of ongoing research, changes in government regulations, and the constant flow of information relating to drug therapy and drug reactions, the reader is urged to check the package insert for each drug for any change in indications and dosage and for added warnings and precautions. This is particularly important when the recommended agent is a new or infrequently employed drug.

Some drugs and medical devices presented in this publication have Food and Drug Administration (FDA) clearance for limited use in restricted research settings. It is the responsibility of the health care provider to ascertain the FDA status of each drug or device planned for use in their clinical practice.

10 9 8 7 6 5 4 3 2 1

Journal of General Virology (1990), **71**, 3075–3080. *Printed in Great Britain*

Heptad repeat sequences are located adjacent to hydrophobic regions in several types of virus fusion glycoproteins

Philip Chambers, Craig R. Pringle and Andrew J. Easton*

Department of Biological Sciences, University of Warwick, Coventry CV4 7AL, U.K.

Extensive regions of heptad repeat units consistent with an α-helical coiled coil conformation are located adjacent to hydrophobic, potentially fusion-related regions in the amino acid sequences of paramyxovirus fusion and retrovirus envelope glycoproteins. Similar arrangements of hydrophobic peptides and heptad repeat units exist in coronavirus peplomer proteins and influenza virus haemagglutinins. This suggests that there may be similarities in the structures of these proteins and in the functions of the hydrophobic fusion-related regions during virus entry.

It has been proposed that many transmembrane proteins may include sections of α-helical coiled coil, in which two or more α-helices associate lengthwise by coiling around each other to maintain contact along hydrophobic faces (Cohen & Philips, 1981; Cohen & Parry, 1986). Coiled coils may form in proteins where extensive regions that are devoid of potential helix-breaking prolines occur, and consist of seven residue (heptad) repeats of amino acids in a sequence periodicity (a b c d e f g) in which the side-chains of amino acids in positions a and d are predominantly bulky and hydrophobic or neutral. These features in amino acid sequences are capable of generating hydrophobic faces on each interacting α-helix, within or between polypeptide chains (Cohen & Parry, 1986; McLachlan & Karn, 1983). The structures of two oligomeric transmembrane glycoproteins, the influenza virus haemagglutinin (HA) and the trypanosome variable surface glycoprotein, include elements of such a supersecondary structure (Wilson *et al.*, 1981, Freymann *et al.*, 1984). Coronavirus peplomer glycoproteins may also contain such a structure (de Groot *et al.*, 1987).

We have determined the nucleotide and deduced amino acid sequences of cDNA clones from pneumonia virus of mice, a paramyxovirus classified in the genus *Pneumovirus* (Chambers *et al.*, 1990). A region containing heptad repeat units was detected in the amino acid sequence of the fusion glycoprotein (Fig. 1). The heptad repeat pattern is conserved in the amino acid sequence of the fusion glycoprotein of another pneumovirus, human respiratory syncytial virus, and also in the amino acid sequences of the fusion glycoproteins of members of the more distantly related *Paramyxovirus* and *Morbillivirus* genera of the family *Paramyxoviridae* (Fig. 1). The heptad repeat regions are relatively poor in glycines, contain no helix-breaking prolines and charged amino acid side-chains are scattered in all heptad positions except a and d. The heptad repeat pattern, shown in Fig. 1, is located in the F1 portion of the paramyxovirus fusion glycoproteins, adjacent to the hydrophobic amino terminus (Fig. 2). Furthermore, the heptad regions of the paramyxovirus fusion glycoproteins shown in Fig. 1 represent that part of the protein which is most similar between paramyxoviruses and pneumoviruses (Fig. 3 in Chambers *et al.*, 1986). A second region of similarity, which is located near the transmembrane domain, also consists of heptad repeats and is discussed below (Buckland & Wild, 1989).

This comparison was extended to the cleavage/activation sequences of retroviruses because similarity between the amino terminus of F1 of respiratory syncytial virus and the envelope glycoprotein of human immunodeficiency virus has been suggested (Gallaher, 1987). A region of heptad repeat units has been located on the carboxy-terminal side of the retroviral cleavage site (Fig. 1 and 2). These heptad repeats commence approximately 20 to 40 amino acids from the cleavage sites in paramyxoviruses and the oncovirus and lentivirus subgroups of the retroviruses. For consistency between the oncovirus and lentivirus sequences, heptad positions a and d are indicated only in the region where most of the aligned residues have bulky side-chains (Cohen & Parry, 1986). Several other paramyxovirus fusion and retrovirus envelope glycoprotein sequences have also been examined; that of equine infectious anaemia virus shown in Fig. 1 is the only sequence identified thus far that contains a charged amino acid residue at any of the heptad positions a or d. Although this is probably un-

0000-9769 © 1990 SGM

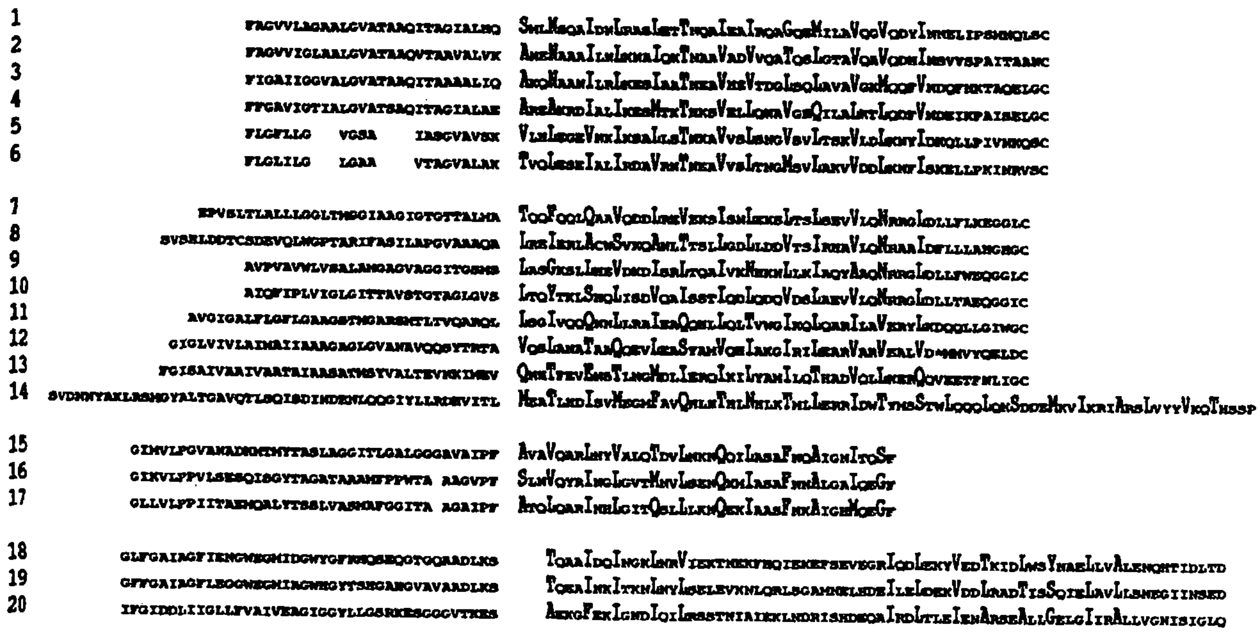

Fig. 1. Amino acid sequences of hydrophobic and adjacent heptad repeat regions in virus fusion glycoproteins. A gap has been inserted into all of the sequences to separate the regions of heptad repeats (to the right of the gap) from the regions containing hydrophobic peptides. 1 to 6, Paramyxovirus fusion proteins; 7 to 14, retrovirus envelope proteins; 15 to 17, coronavirus peplomer proteins; 18 to 20 influenza virus haemagglutinins. Sequences 1 to 14 and 18 to 20 commence at the known or deduced cleavage/activation sites of the glycoproteins. 1. Measles virus (genus *Morbillivirus*) residues 113 to 195, Richardson *et al.* (1986). 2. Simian virus 5 (genus *Paramyxovirus*), residues 103 to 185, Paterson *et al.* (1984). 3. Newcastle disease virus (genus *Paramyxovirus*), residues 117 to 199, Chambers *et al.* (1986). 4. Sendai virus (genus *Paramyxovirus*), residues 117 to 199, Blumberg *et al.* (1985). 5. Respiratory syncytial virus (genus *Pneumovirus*), residues 137 to 212, Collins *et al.* (1984). 6. Pneumonia virus of mice (genus *Pneumovirus*), residues 102 to 177, P. Chambers *et al.* (unpublished results). 7. Moloney leukaemia virus (genus *Oncovirus*), residues 470 to 555, Shinnick *et al.* (1981). 8. Rous sarcoma virus (genus *Oncovirus*), residues 404 to 493, Hunter *et al.* (1983). 9. Human T cell leukaemia virus type 1 (genus *Oncovirus*), residues 313 to 393, Seiki *et al.* (1983). 10. Simian retrovirus type 1 (genus *Oncovirus*), residues 414 to 494, Power *et al.* (1986). 11. Human immunodeficiency virus (genus *Lentivirus*), residues 517 to 603, Wain-Hobson *et al.* (1985). 12. Visna virus (genus *Lentivirus*), residues 657 to 745, Sonigo *et al.* (1985). 13. Equine infectious anaemia virus (genus *Lentivirus*), residues 446 to 535, Rushlow *et al.* (1986). 14. Human spumavirus (genus *Spumavirus*), residues 569 to 694, Flugel *et al.* (1987). 15. Transmissible gastroenteritis virus, residues 999 to 1077, Rasschaert & Laude (1987). 16. Murine hepatitis virus, residues 822 to 899, Schmidt *et al.* (1987). 17. Infectious bronchitis virus, residues 734 to 811, Binns *et al.* (1985). 18. Influenza A virus, residues 346 to 457, Verhoeyen *et al.* (1980). 19. Influenza B virus, residues 362 to 473, Krystal *et al.* (1982). 20. Influenza C virus, residues 446 to 557, Nakada *et al.* (1984). For convenience, heptad regions are aligned on the first position of the most plausible series following the hydrophobic peptides, except in the influenza haemagglutinins (18 to 20) where this first position is not part of the shorter stem helix (Wilson *et al.*, 1981). Residues in heptad positions a and d are in larger type. The asterisk in the visna virus sequence (12) corresponds to a stop codon presumed by Sonigo *et al.* (1985) to result from cloning of a defective genome.

favourable, there are many precedents for the presence of polar (N and Q) or charged (K, R or E; D is rare) amino acid side-chains in heptad positions a or d (McLachlan & Karn, 1983). Statistically, there is a highly significant association by the χ^2 test of hydrophobic amino acids (I, L, V, M, F and Y) in heptad positions a and d for paramyxovirus and retrovirus sequences in the regions indicated in Fig. 1 (data not shown). It seems unlikely that the regions of heptad repeats described above are present by chance in all of these glycoproteins because extensive patterns of heptad repeats have not been detected in multiple alignments of other paramyxovirus proteins (Rima, 1989) or in alignments of sequences from proteins of known non-coiled coil structure (influenza virus HA head region, Hiti *et al.*, 1981; influenza virus neuraminidase, Air *et al.*, 1985; haemoglobin, Barton & Sternberg, 1987).

Potential long α-helices formed by these heptad repeat regions may be terminated at the site of the first proline residue, which is conserved in most of the paramyxovirus sequences, or the paired glycines, the presence and approximate location of which are conserved in most of the retroviral sequences. These potential breaks are closely followed by conserved cysteines which may be involved in disulphide bond formation with the other peptide of the fusion protein monomer (Buckland *et al.*,

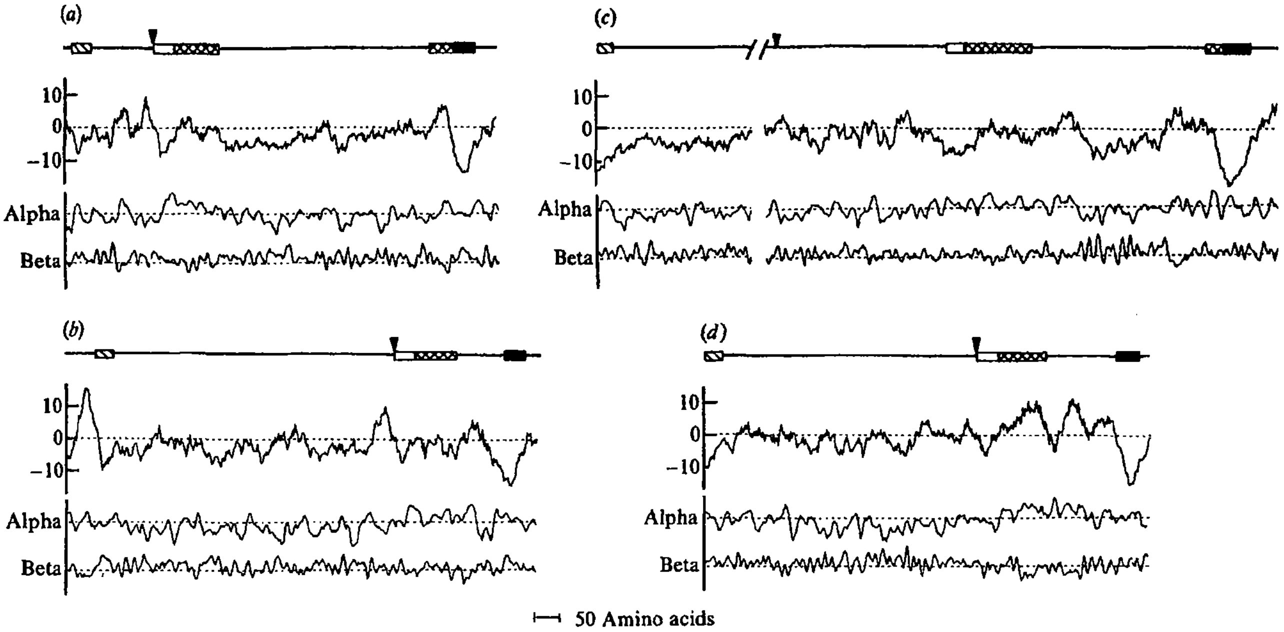

Fig. 2. Location of hydrophobic and heptad repeat regions in virus fusion glycoproteins. Also shown are the predicted probabilities of α-helix and β-sheet structure (Garnier *et al.*, 1978) and the hydrophobicity profiles (Hopp & Woods, 1981), with a window of 20 residues, determined using the Microgenie sequence analysis program (Beckman Instruments). The key beneath the figure indicates the scale, cleavage/activation sites, heptad repeat regions and hydrophobic signal, transmembrane and potential fusion-related regions. A representative paramyxovirus (Newcastle disease virus, *a*), retrovirus (Rous sarcoma virus, *b*), coronavirus (infectious bronchitis virus, *c*) and influenza A virus (A/Aichi/2/68, *d*) is indicated. From the amino terminus at the left, the Newcastle disease virus protein is cleaved into F2 and F1 portions the Rous sarcoma virus protein is cleaved into gp85 and gp37 portions, the infectious bronchitis virus protein is cleaved into S1 and S2 portions and the influenza A virus protein is cleaved into HA1 and HA2 portions. For display purposes, a break has been introduced into the infectious bronchitis virus S1 portion, which is 537 amino acids in length. ▨, Signal sequence; ▼, cleavage site; ■, transmembrane region; ▩, heptad region; □, fusion-related region.

1987; Shinnick *et al.*, 1981). The spumavirus subgroup of the retroviruses differs somewhat in that a rather longer region of heptad repeats commences 49 residues from the proposed cleavage site (Fig. 1). Paramyxovirus fusion glycoproteins and retroviral envelope glycoproteins are thought to be oligomeric (Sechoy *et al.*, 1987; Pinter & Fleissner, 1979; Pepinsky *et al.*, 1980) and therefore regions of heptad repeats may be of great structural importance if they form α-helical coiled coils between the subunits.

Heptad repeat regions have also been described in coronavirus peplomer glycoprotein sequences (de Groot *et al.*, 1987). For simplicity, coronavirus sequences are displayed in Fig. 1 showing the phasing of heptads adjacent to the hydrophobic regions described below, extending only until it becomes necessary to position gaps to align similar sequences. A further parallel between the coronavirus peplomer and paramyxovirus fusion glycoprotein sequences is the presence of a second series of heptad repeats immediately adjacent to the presumed transmembrane domain of all of these glycoproteins (de Groot *et al.*, 1987; Buckland & Wild, 1989). The corresponding regions of the paramyxovirus fusion proteins contain heptad repeats which have been likened to a leucine zipper motif (Buckland & Wild, 1989; Landschultz *et al.*, 1988), which may form part of a helical bundle, interacting with the longer heptad regions shown in Fig. 1 to stabilize the base of fusion protein oligomers. This has been proposed for coronaviruses and is demonstrated in the trypanosome variable surface glycoprotein (de Groot *et al.*, 1987; Freymann *et al.*, 1984). Retrovirus envelope glycoprotein sequences also contain short regions predicted to be helical adjacent to the transmembrane domain but no extended patterns of heptads are conserved.

Hydrophobicity and predicted α-helical and β-sheet structure profiles of representative paramyxo-, retro-, corona- and influenza viruses are shown in Fig. 2. The heptad repeat regions are predicted to be largely α-helical in all these cases (and also for other representatives of these virus groups; not shown). Studies using circular dichroism also suggest that paramyxovirus fusion proteins contain large amounts of α-helical secondary structure (Hsu *et al.*, 1982). The heptad regions of paramyxovirus fusion and coronavirus peplomer glycoproteins are reasonably hydrophilic despite the regular pattern of hydrophobic amino acids in positions a and d, consistent with the formation of an extended structure (Cohen & Parry, 1986). The heptad regions of some retroviruses, for example human immunodeficiency virus (not shown), are somewhat more hydrophobic, suggesting that they may be less exposed to solvent than those of the other examples shown.

Heptad repeat regions have been detected in several other virus glycoprotein sequences. Glycoprotein gB of herpes simplex virus, and its homologues in other herpesviruses, contains a short run of heptad repeats that continues into a non-heptad region predicted to be helical (herpes simplex virus residues 502 to 546; Bzik *et al.*, 1984; Pellett *et al.*, 1985); in arenaviruses the glycoprotein precursor contains a reasonably long run of heptad repeats with a high prediction of an α-helix (Lassa virus residues 309 to 346; Auperin *et al.*, 1986). Again, residues adjacent to membrane-associated regions are hydrophilic and predicted to be in a helical conformation (not shown).

Hydrophobic regions thought to be involved in virus entry and cell fusion are located between the cleavage/activation site and the heptad repeat regions in both paramyxo- and retroviruses (Fig. 2). Similarity can be detected amongst all paramyxoviruses if gaps are inserted into the pneumovirus sequences (Fig. 1). These hydrophobic regions also have sequences consistent with predictions of an α-helix (Server *et al.*, 1985; Richardson *et al*, 1986) but, if the heptad pattern is simply extended back towards the cleavage site, positions a and d would be predominantly occupied by glycine or alanine rather than the bulkier hydrophobic residues preferred in these positions in α-helical coiled coils (Cohen & Parry, 1986). In contrast, the hydrophobic sequences between cleavage sites and the heptad repeat regions of the retroviral glycoproteins are quite diverse. Cleavage is not required for fusion activity of coronaviruses and there is no hydrophobic region adjacent to the cleavage site (Spaan *et al.*, 1988). There is, however, a hydrophobic region on the amino-terminal side of the longer area of heptad repeats, as in paramyxovirus and retrovirus glycoproteins (Fig. 1 and 2). By analogy to paramyxo- and retroviruses, these regions may function in virus entry and cell fusion. These hydrophobic regions in the retro- and coronavirus glycoproteins are usually rich in alanine and turn-inducing amino acid residues (glycines or prolines).

These predicted features have some similarities to the known structure of the influenza virus HA, the virus fusion protein (Huang *et al.*, 1980). The HA is a trimer built around a bundle of α-helices. It is primed for function by proteolytic cleavage which generates a new, glycine-rich, hydrophobic amino terminus on the HA2 peptide (Fig. 2) but is not proficient in fusion until a conformational change is induced by incubation at acid pH (Wilson *et al.*, 1981; Klenk *et al.*, 1975; Waterfield *et al.*, 1979; Skehel *et al.*, 1982). The amino acid sequences of the HA2s continue with two series of heptad repeats (compressed to one region in Fig. 2); the first corresponds to the shorter helices of the stem, the second corresponds to the inner surface at the top of the longer helices where they make close (1 nm) contact. The conformational change necessary to activate the protein at pH 5 may involve upward movement by the shorter stem helices to form the knob which appears at the top of the stem and might therefore contain elements of anti-parallel α-helical coiled coil (Ruigrok *et al.*, 1986).

In conclusion, heptad repeats may be associated with the presence of long, inter-subunit, α-helical coiled coils which could form the backbones of the projections or spikes on the viral envelopes, as predicted previously in general terms and demonstrated in influenza virus HA and (in a non-viral example) the trypanosome variable surface glycoprotein (Cohen & Philips, 1981; Wilson *et al.*, 1981; Freymann *et al.*, 1984). The heptad repeat regions shown in Fig. 1 may form a single long helix in paramyxoviruses and retroviruses. The hydrophobic regions that are located at the amino-terminal ends of the heptad repeat regions (Fig. 2) are thought to function in virus entry and cell fusion (Gething *et al.*, 1978; Richardson *et al.*, 1980; Shinnick *et al.*, 1981). Assuming that the proposed long helices are oriented more or less perpendicular to the viral membrane, the hydrophobic regions would be in position to function during virus entry. If the amino terminus of the long helix pointed away from the virus core, the hydrophobic region could interact with, and perhaps destabilize, the cell membrane; if it pointed towards the core, it could interact with the viral membrane. If the subunit interface of the virus fusion proteins can form a hydrophobic channel, lipid movements between membranes to be fused may be allowed. Thus, diverse groups of enveloped viruses may have developed similar structures to enable the fusion of virus and cellular membranes.

References

AIR, G. M., RITCHIE, L. R., LAVER, W. G. & COLMAN, P. M. (1985). Gene and protein sequence of an influenza neuraminidase with hemagglutinin activity. *Virology* **145**, 117–122.

AUPERIN, D. D., SASSO, D. R. & MCCORMICK, J. B. (1986). Nucleotide sequence of the glycoprotein gene and intergenic region of the Lassa virus S genome RNA. *Virology* **154**, 155–167.

BARTON, G. J. & STERNBERG, M. J. E. (1987). A strategy for the rapid multiple alignment of protein sequences. Confidence levels from tertiary structure comparisons. *Journal of Molecular Biology* **198**, 327–337.

Binns, M. M., Boursnell, M. E. G., Cavanagh, D., Pappin, D. J. C. & Brown, T. D. K. (1985). Cloning and sequencing of the gene encoding the spike protein of the coronavirus IBV. *Journal of General Virology* **66**, 719–726.

Blumberg, B. M., Giorgi, C., Rose, K. & Kolakofsky, D. (1985). Sequence determination of the Sendai virus fusion protein gene. *Journal of General Virology* **66**, 317–331.

Buckland, R. & Wild, F. (1989). Leucine zipper motif extends. *Nature, London* **338**, 547.

Buckland, R., Gerald, C., Barker, R. & Wild, T. F. (1987). Fusion glycoprotein of measles virus: nucleotide sequence of the gene and comparison with other paramyxoviruses. *Journal of General Virology* **68**, 1695–1703.

Bzik, D. J., Fox, B. A., DeLuca, N. A. and Person, S. (1984). Nucleotide sequence specifying the glycoprotein gene gB of herpes simplex virus type 1. *Virology* **133**, 301–314.

Chambers, P., Millar, N. S. & Emmerson, P. T. (1986). Nucleotide sequence of the gene encoding the fusion glycoprotein of Newcastle disease virus. *Journal of General Virology* **67**, 2685–2694.

Chambers, P., Barr, J., Pringle, C. R. & Easton, A. J. (1990). Molecular cloning of pneumonia virus of mice. *Journal of Virology* **64**, 1869–1872.

Cohen, C. & Parry, D. A. D. (1986). α helical coiled coils: a widespread motif in proteins. *Trends in Biochemical Sciences* **11**, 245–248.

Cohen, C. & Philips, G. N. (1981). Spikes and fimbriae: α helical proteins form surface projections on microorganisms. *Proceedings of the National Academy of Sciences, U.S.A.* **78**, 5303–5304.

Collins, P. L., Huang, Y. T. & Wertz, G. W. (1984). Nucleotide sequence of the gene encoding the fusion F glycoprotein of human respiratory syncytial virus. *Proceedings of the National Academy of Sciences, U.S.A.* **81**, 7683–7687.

de Groot, R. J., Luytjes, W., Horzinek, M. C., van der Zeijst, B.A.M., Spaan, W. J. M. & Lenstra, J.A. (1987). Evidence for a coiled coil structure in the spike proteins of coronaviruses. *Journal of Molecular Biology* **196**, 963–966.

Flugel, R. M., Rethwilm, A., Maurer, B. & Darai, G. (1987). Nucleotide sequence analysis of the *env* gene and its flanking regions of the human spumaretrovirus reveals two novel genes. *EMBO Journal* **6**, 2077–2084.

Freymann, D. M., Metcalf, P., Turner, M. & Wiley, D. C. (1984). 6Å resolution X-ray structure of a variable surface glycoprotein from *Trypanosoma brucei*. *Nature, London* **311**, 167–169.

Gallaher, W. R. (1987). Detection of a fusion peptide sequence in the transmembrane protein of human immunodeficiency virus. *Cell* **50**, 327–328.

Garnier, J., Osguthorpe, D. J. & Robson, B. (1978). Analysis of the accuracy and implications of simple methods for predicting the secondary structure of globular proteins. *Journal of Molecular Biology* **120**, 97–120.

Gething, M. J., White, J. M. & Waterfield, M. D. (1978). Purification of the fusion protein of Sendai virus: analysis of the NH_2-terminal sequence generated during precursor activation. *Proceedings of the National Academy of Sciences, U.S.A.* **75**, 2737–2740.

Hiti, A. L., Davis, A. R. & Nayak, D. P. (1981). Complete sequence analysis shows that the hemagglutinin of the H0 and H2 subtypes of human influenza virus are closely related. *Virology* **111**, 113–124.

Hopp, T. P. & Woods, K. R. (1981). Prediction of protein antigenic determinants from amino acid sequences. *Proceedings of the National Academy of Sciences, U.S.A.* **78**, 3824–3828.

Hsu, M.-C., Scheid, A. & Choppin, P. W. (1982). Enhancement of membrane-fusion activity of Sendai virus by exposure of the virus to basic pH is correlated with a conformational change in the fusion protein. *Proceedings of the National Academy of Sciences, U.S.A.* **79**, 5862–5866.

Huang, R. T. C., Wahn, K., Klenk, H.-D. & Rott, R. (1980). Fusion between cell membranes and liposomes containing the glycoproteins of influenza virus. *Virology* **104**, 294–302.

Hunter, E., Hill, E., Hardwick, M., Bhowm, A., Schwartz, D. E. & Tizard, R. (1983). Complete sequence of the Rous sarcoma virus *env* gene: identification of structural and functional regions of its product. *Journal of Virology* **46**, 920–936.

Klenk, H.-D., Rott, R., Ohrlich, M. & Blodorn, J. (1975). Activation of influenza viruses by trypsin treatment. *Virology* **68**, 426–429.

Krystal, M., Elliott, R. M., Bey, E. W., Young, J. F. & Palese, P. (1982). Evolution of influenza A and B viruses: conservation of structural features in the hemagglutinin genes. *Proceedings of the National Academy of Sciences, U.S.A.* **79**, 4800–4804.

Landschultz, W. H., Johnson, P. F. & McKnight, S. L. (1988). The leucine zipper: a hypothetical structure common to a new class of DNA binding proteins. *Science* **240**, 1759–1764.

McLachlan, A. D. & Karn, J. (1983). Periodic features in the amino acid sequence of nematode myosin rod. *Journal of Molecular Biology* **164**, 605–626.

Nakada, S., Creager, R. S., Krystal, M., Aaronson, R. P. & Palese, P. (1984). Influenza C virus hemagglutinin: comparison with influenza A and B virus hemagglutinins. *Journal of Virology* **50**, 118–124.

Paterson, R. G., Harris, T. J. R. & Lamb, R. A. (1984). Fusion protein of the paramyxovirus simian virus 5: nucleotide sequence of the mRNA predicts a highly hydrophobic glycoprotein. *Proceedings of the National Academy of Sciences, U.S.A.* **81**, 6706–6710.

Pellett, P. E., Biggin, M. D., Barrell, B. & Roizman, B. (1985). Epstein–Barr virus genome may encode a protein showing significant amino acid and predicted secondary structure homology with glycoprotein B of herpes simplex virus 1. *Journal of Virology* **56**, 807–813.

Pepinsky, R. B., Cappiello, D., Wilkowski, C. & Vogt, V. M. (1980). Chemical cross-linking of proteins in avian sarcoma and leukemia viruses. *Virology* **102**, 205–210.

Pinter, A. & Fleissner, E. (1979). Structural studies of retroviruses: characterization of oligomeric complexes of murine and feline leukemia virus envelope and core components formed upon cross-linking. *Journal of Virology* **30**, 157–165.

Power, M. D., Marx, P. A., Bryant, M. L., Gardner, M. B., Barr, P. J. & Luciw, P. A. (1986). Nucleotide sequence of SRV1, a type D simian acquired immune deficiency syndrome retrovirus. *Science* **231**, 1567–1572.

Rasschaert, D. & Laude, H. (1987). The predicted primary structure of the peplomer protein E2 of the porcine coronavirus transmissible gastroenteritis virus. *Journal of General Virology* **68**, 1883–1890.

Richardson, C., Hull, D., Greer, P., Hasel, K., Berkovich, A., Englund, G., Bellini, W., Rima, B. & Lazzarini, R. (1986). The nucleotide sequence of the mRNA encoding the fusion protein of measles virus (Edmonston strain): a comparison of fusion proteins from several different paramyxoviruses. *Virology* **155**, 508–523.

Richardson, C. D., Scheid, A. & Choppin, P. W. (1980). Specific inhibition of paramyxovirus and myxovirus replication by oligopeptides with amino acid sequences similar to those at the N-termini of the F1 or HA2 viral polypeptides. *Virology* **105**, 205–222.

Rima, B. (1989). Comparison of amino acid sequences of the major structural proteins of the paramyxo- and morbilliviruses. In *Genetics and Pathogenicity of Negative Strand Viruses*, pp. 254–263. Edited by D. Kolakofsky & B. W. J. Mahy. Amsterdam: Elsevier.

Ruigrok, R. W. H., Wrigley, N. G., Calder, L. J., Cusack, S., Wharton, S. A., Brown, E. B. & Skehel, J. J. (1986). Electron microscopy of the low pH structure of influenza virus haemagglutinin. *EMBO Journal* **5**, 41–49.

Rushlow, K., Olsen, K., Stiegler, G., Payne, S. L., Montelaro, R. C. & Issel, C. J. (1986). Lentivirus genomic organization: the complete nucleotide sequence of the *env* gene region of equine infectious anemia virus. *Virology* **155**, 309–321.

Schmidt, I., Skinner, M. & Siddell, S. (1987). Nucleotide sequence of the gene encoding the surface projection glycoprotein of coronavirus MHV-JHM. *Journal of General Virology* **68**, 47–56.

Sechoy, O., Philippot, J. R. & Bienvenue, A. (1987). F protein-F protein interaction within the Sendai virus identified by native bonding or chemical cross-linking. *Journal of Biological Chemistry* **262**, 11519–11523.

Seiki, M., Hattori, S., Hirayama, Y. & Yoshida, M. (1983). Human adult T-cell leukemia virus: complete nucleotide sequence of the provirus genome integrated in leukemia cell DNA. *Proceedings of the National Academy of Sciences, U.S.A.* **80**, 3618–3622.

Server, A. C., Smith, J. A., Waxham, M. N., Wolinsky, J. S. & Goodman, H . M. (1985). Purification and amino-terminal protein sequence analysis of the mumps virus fusion protein. *Virology* **144**, 373–383.

Shinnick, T. N., Lerner, R. A. & Sutcliffe, J. G. (1981). Nucleotide sequence of Moloney murine leukaemia virus. *Nature, London* **293**, 543–548.

Skehel, J. J., Bayley, P. M., Brown, E. B., Martin, S. R., Waterfield, M. D., White, J. M., Wilson, I. A. & Wiley, D. C. (1982). Changes in the conformation of influenza virus hemagglutinin at the pH optimum of virus-mediated membrane fusion. *Proceedings of the National Academy of Sciences, U.S.A.* **79**, 968–972.

Sonigo, P., Alizon, M., Staskus, K., Klatzman, D., Cole, S., Danos, O., Retzel, E., Tiollais, P., Haase, A. & Wain-Hobson, S. (1985). Nucleotide sequence of the visna lentivirus: relationship to the AIDS virus. *Cell* **42**, 369–382.

Spaan, W., Cavanagh, D. & Horzinek, M. C. (1988). Coronaviruses: structure and genome expression. *Journal of General Virology* **69**, 2939–2952.

Verhoeyen, M., Fang, R., Min Jou, W., Devos, R., Huylebroeck, D., Saman, E. & Fiers, W. (1980). Antigenic drift between the haemagglutinin of the Hong Kong influenza strains A/Aichi/2/68 and A/Victoria/3/75. *Nature, London* **286**, 771–776.

Wain-Hobson, S., Sonigo, P., Danos, O., Cole, S. & Alizon, M. (1985). Nucleotide sequence of the AIDS virus, LAV. *Cell* **40**, 9–17.

Waterfield, M. D., Espelie, K., Elder, K. & Skehel, J. J. (1979). Structure of the haemagglutinin of influenza virus. *British Medical Bulletin* **35**, 5763.

Wilson, I. A., Skehel, J. J. & Wiley, D. C. (1981). Structure of the haemagglutinin membrane glycoprotein of influenza virus at 3Å resolution. *Nature, London* **289**, 366–373.

(*Received 26 June 1990; Accepted 28 August 1990*)

NCBI PubMed www.pubmed.gov
A service of the National Library of Medicine and the National Institutes of Health
My NCBI
[Sign In] [Regis

All Databases PubMed Nucleotide Protein Genome Structure OMIM PMC Journals Book

Search PubMed for Go Clear

☑ Limits Preview/Index History Clipboard Details

Field: Title/Abstract

Display AbstractPlus Show 20 Sort By Send to

All: 1 Review: 0

1: J Virol. 1998 Mar;72(3):1959-66.

Final Version FREE J Virol
FREE full text article in PubMed Central
Links

Erratum in:
J Virol 1998 Jul;72(7):6278.

Identification of a domain within the human T-cell leukemia virus type 2 envelope required for syncytium induction and replication.

Poon B, **Chen IS**.

Department of Microbiology and Immunology, UCLA School of Medicine, Los Angeles, California 90095, USA.

In vitro infection by human T-cell leukemia virus type 1 and 2 (HTLV-1 and HTLV-2) can result in syncytium formation, facilitating viral entry. Using cell lines that were susceptible to HTLV-2-mediated syncytium formation but were nonfusogenic with HTLV-1, we constructed chimeric envelopes between HTLV-1 and -2 and assayed for the ability to induce syncytia in BJAB cells and HeLa cells. We have identified a fusion domain composed of the first 64 amino acids at the amino terminus of the HTLV-2 transmembrane protein, p21, the retention of which was required for syncytium induction. Construction of replication-competent HTLV genomic clones allowed us to correlate the ability of HTLV-2 to induce syncytia with the ability to replicate in BJAB cells. Differences in the ability to induce syncytia were not due to differences in the levels of total or cell membrane-associated envelope or in the formation of multimers. Therefore, we have localized a fusion domain within the amino terminus of the transmembrane protein of HTLV-2 envelope that is necessary for syncytium induction and viral replication.

PMID: 9499049 [PubMed - indexed for MEDLINE]

Related Links

Molecular cloning, expression, and biological characterization of an HTLV-II envelope glycoprotein: HIV-1 expression is permissive for HTLV-II-induced [AIDS Res Hum Retroviruses. 1993]

Human T-cell leukemia virus type 1 receptor expression among syncytium-resistant cell lines revealed by a novel surface glycoprotein-immu [J Virol. 2001]

Analysis of functional conservation in the surface and transmembrane glycoprotein subunits of human T-cell leukemia virus type 1 (HTLV-1) and HTLV-2. [J Virol. 1998]

Human T-cell leukemia virus type 1 envelope-mediated syncytium formation can be activated in resistant Mammalian cell lines by a carboxy-terminal truncation of the envelope cytoplasmic domain. [J Virol. 2003]

Syncytium formation by recombinant HTLV-II envelope glycop [Virology. 1996]

See all Related Articles...

Display AbstractPlus Show 20 Sort By Send to

Write to the Help Desk
NCBI | NLM | NIH
Department of Health & Human Services
Privacy Statement | Freedom of Information Act | Disclaimer

JOURNAL OF VIROLOGY, Aug. 1999, p. 6782–6790
0022-538X/99/$04.00+0
Copyright © 1999, American Society for Microbiology. All Rights Reserved.
Vol. 73, No. 8

Functional Analysis of Cell Surface-Expressed Hepatitis C Virus E2 Glycoprotein

MIKE FLINT,[1] JOANNE M. THOMAS,[1] CATHERINE M. MAIDENS,[1] CHRISTINE SHOTTON,[2]
SHOSHANA LEVY,[3] WENDY S. BARCLAY,[1] AND JANE A. McKEATING[1]*

School of Animal and Microbial Sciences, University of Reading, Whiteknights, Reading RG6 6AJ,[1] and Institute for Cancer Research, Sutton SM2 5NG,[2] United Kingdom, and Department of Medicine, Division of Oncology, Stanford University Medical Center, Stanford, California 94305[3]

Received 6 November 1998/Accepted 29 March 1999

Hepatitis C virus (HCV) glycoproteins E1 and E2, when expressed in eukaryotic cells, are retained in the endoplasmic reticulum (ER). C-terminal truncation of E2 at residue 661 or 715 (position on the polyprotein) leads to secretion, consistent with deletion of a proposed hydrophobic transmembrane anchor sequence. We demonstrate cell surface expression of a chimeric glycoprotein consisting of E2 residues 384 to 661 fused to the transmembrane and cytoplasmic domains of influenza A virus hemagglutinin (HA), termed $E2_{661}$-HA_{TMCT}. The $E2_{661}$-HA_{TMCT} chimeric glycoprotein was able to bind a number of conformation-dependent monoclonal antibodies and a recombinant soluble form of CD81, suggesting that it was folded in a manner comparable to "native" E2. Furthermore, cell surface-expressed $E2_{661}$-HA_{TMCT} demonstrated pH-dependent changes in antigen conformation, consistent with an acid-mediated fusion mechanism. However, $E2_{661}$-HA_{TMCT} was unable to induce cell fusion of CD81-positive HEK cells after neutral- or low-pH treatment. We propose that a stretch of conserved, hydrophobic amino acids within the E1 glycoprotein, displaying similarities to flavivirus and paramyxovirus fusion peptides, may constitute the HCV fusion peptide. We demonstrate that influenza virus can incorporate $E2_{661}$-HA_{TMCT} into particles and discuss experiments to address the relevance of the E2-CD81 interaction for HCV attachment and entry.

Enveloped viruses acquire their lipid membranes by budding through host cellular membranes (reviewed in reference 35). The majority of enveloped viruses bud at the plasma membrane. However, several viruses assemble and bud at internal membranes such as those of the endoplasmic reticulum (ER) (e.g., rotaviruses), ER-Golgi intermediate compartments (e.g., coronaviruses), or the Golgi complex (e.g., bunyaviruses). This behaviour generally reflects the targeting of the viral glycoproteins (gps) within subcompartments of the ER or Golgi complex. In the latter cases, viruses are released from infected cells either by cell lysis or after transport through the cellular secretory pathway to the cell surface.

Hepatitis C virus (HCV), the major cause of non-A, non-B hepatitis, is an enveloped virus classified in the *Flaviviridae* family (reviewed in references 3 and 39). The genome encodes two putative envelope gps, E1 (polyprotein residues 192 to 383) and E2 (residues 384 to 746), which are released from the viral polyprotein by signal peptidase cleavage(s) (13, 18, 43). Both gps are heavily modified by N-linked glycosylation and are believed to be type I integral transmembrane proteins, with C-terminal hydrophobic anchor domains.

Expression of the E1E2 gps in mammalian cell lines demonstrates their ER retention with no cell surface gp expression detectable (8, 37, 46, 47). Immunoelectron microscopic studies localized the gps to the ER (7, 8). We (10) and others (4) reported the presence of ER retention "signals" within the C-terminal regions of both E1 and E2 gps, explaining these observations. Consistent with these data, truncation of E2 at its C terminus leads to its secretion from expressing cells (26, 29, 30, 45, 47). These observations are consistent with a model of HCV particle morphogenesis occurring by budding into the ER, as reported for other members of the *Flaviviridae*.

When expressed in tissue culture cells, the E1 and E2 gps interact to form noncovalently linked complexes, whose size is consistent with E1E2 heterodimers (6, 8). In addition to these noncovalently associated E1E2 complexes, a significant proportion of E1 and E2 are present in disulfide-linked aggregates, which are believed to result from a nonproductive folding pathway (1a, 6, 8, 13). Since HCV cannot be propagated efficiently in vitro, it has been difficult to study "native" E1E2 gp forms as they exist on the virus particle. It is critical when studying the biological activity of the HCV gps to distinguish between molecules that undergo productive folding and assembly and those that follow a nonproductive pathway(s) resulting in misfolding and aggregation (7). Recently, Dubuisson and colleagues reported a number of conformation-dependent monoclonal antibodies (MAbs) (H2 and H53) which specifically recognize nondisulfide-bridged E2, both alone and when complexed with E1, allowing the study of gp complexes which may represent "native" prebudding forms of the HCV gp complex (4, 6, 30).

gps exposed on the virus surface mediate entry into target cells. This process requires binding of the virus particle to a receptor(s) present at the surface of the host cell, followed by fusion of the viral and cellular membranes. For viruses such as influenza virus and the flavivirus tick-borne encephalitis virus, particles internalize after receptor binding and fuse with the endosomal membranes. The low pH within the endosomal compartment induces a major structural rearrangement of the gps, resulting in exposure of a fusion peptide which destabilizes membranes, leading to fusion (reviewed in references 11, 17, and 50). The mechanism by which HCV enters target cells is currently unknown; however, the E2 gp is thought to be responsible for initiating virus attachment to a receptor on po-

---

* Corresponding author. Mailing address: School of Animal and Microbial Sciences, University of Reading, Whiteknights, P.O. Box 228, Reading RG6 6AJ, United Kingdom. Phone: (44) 1189 875 123, ext. 7892/4275. Fax: (44) 1189 316 671. E-mail: j.a.mckeating@reading.ac.uk.

tential host cells (42). Indeed, a soluble form of a C-terminally truncated E2 gp was used to identify CD81 as a putative receptor for HCV (36). CD81 is a broadly expressed protein and is reported to be involved in a variety of biological responses including adhesion, morphology, proliferation, activation, and differentiation of T-, B-, and other cell types (reviewed in reference 23).

Generation of viral pseudotypes is one of the most widely used methods for assaying functional receptors, allowing attachment, penetration, and uncoating to be studied. Recent reports that vesicular stomatitis virus (VSV) expressing chimeric HCV E2 gps, comprising the putative E2 ectodomain fused to the transmembrane and cytoplasmic domains of VSV G protein, allowed entry into target cells suggested that the ectodomain of E2 was sufficient to confer viral attachment and entry (22, 28). We were interested in studying the antigenic conformation of E2 expressed at the cell surface and whether such a protein was able to induce CD81-dependent cell fusion. Here, we demonstrate cell surface expression of a chimeric gp consisting of E2 residues 384 to 661 fused to the transmembrane and cytoplasmic domains of influenza A virus hemagglutinin (HA) (E2$_{661}$-HA$_{\mathrm{TMCT}}$). These data are consistent with a previous report demonstrating cell surface expression of truncated versions of E2 fused to the transmembrane domain of CD4 or a glycosylphosphatidylinositol anchor (4). The E2$_{661}$-HA$_{\mathrm{TMCT}}$ chimeric gp was able to bind a number of conformation-dependent MAbs and a recombinant soluble form of CD81, suggesting that it was folded in a manner comparable to that of native E2. Furthermore, cell surface-expressed E2$_{661}$-HA$_{\mathrm{TMCT}}$ demonstrated pH-dependent changes in antigen conformation, consistent with an acid-mediated fusion mechanism. However, E2$_{661}$-HA$_{\mathrm{TMCT}}$ was unable to induce cell fusion of CD81-positive HEK cells after neutral- or low-pH treatment. We demonstrate that influenza virus can incorporate E2$_{661}$-HA$_{\mathrm{TMCT}}$ into particles and discuss possible experiments to address the relevance of the E2-CD81 interaction for HCV attachment and entry.

MATERIALS AND METHODS

Materials. MAbs specific for E1 (3/8d and 3/8ow), E2 (1/39, 6/82a, and 6/16), CD81 (5A6 [33]), and glutathione *S*-transferase (GST) (2/18) were raised by standard procedures. MAbs specific for conformation-dependent epitopes (H2, H31, H33, H44, H50, H53, H60, and H61) were a gift from J. Dubuisson (Institut Pasteur, Lille, France). MAbs specific for influenza A virus NP and fluorescein isothiocyanate (FITC)-, phycoerythrin (PE)- and horseradish peroxidase (HRP)-conjugated antibodies were purchased from Harlan Sera-Labs. The MAb against MHC class I was purchased from Sigma. Enzymes used for cloning were purchased from Gibco-BRL Life Technologies or New England Biolabs. Dulbecco's minimum essential medium (DMEM), fetal calf serum (FCS), HEPES, and L-glutamine were obtained from Gibco-BRL Life Technologies.

Construction of recombinant cDNA. A cDNA cassette allowing replacement of the ectodomain or transmembrane and cytoplasmic domains of influenza A virus HA was constructed. Unique restriction sites were introduced into the cDNA of HA by PCR mutagenesis. PCR was carried out with sense (W5506; 5′-TCTGGATACAAAGACTGGGCCCTGTGGATTTCCTTTGCC-3′) and antisense (W5501; 5′-GGGCCCCTGCAGGTCGACTCAAATGCAAATGTTGCA-3′) primers on the plasmid pGEM1+HA template (X-31 strain; kindly supplied by D. Steinhauer, National Institute for Medical Research, London, United Kingdom). The resulting product was used as a primer in a secondary reaction with sense primer (W5502; 5′-GGGCCCGATATCAGCAAAAGCAGGGGATAATTC-3′) with pGEM1+HA as the template. The product of this secondary reaction was digested with *Eco*RV and *Pst*I and ligated with pBluescript SK(+) (Stratagene) similarly digested. DNA sequencing of the resulting plasmid, designated pBS+HA/CAS, confirmed the introduction of the unique restriction sites. The vector pCDM8 (Invitrogen) was used for expression in eukaryotic cells. The *Apa*I site within the polyomavirus ori of pCDM8 was destroyed through digestion with *Apa*I, treatment with T4 DNA polymerase, and self-ligation to form pCDM8(−ApaI). Plasmid pBS+HA/CAS was digested with *Hin*dIII and *Pst*I. This fragment was ligated with pCDM8(−ApaI) similarly digested, to form plasmid pCDM8(−ApaI)+HA/CAS(HindIII-PstI). This plasmid was used to generate the fusion protein between the E2 and HA transmembrane and cytoplasmic domain sequences. HCV E2 sequence was amplified by PCR with plasmid pBRTM/HCV1-3011 (kindly supplied by C. M. Rice, Washington University, St. Louis, Mo.) as the template. The sequence encoding HCV residues 364 to 661 was amplified with sense (E2/FWD; 5′-GCGCAAGCTTCCATGGTGGGGAACTGG-3′) and antisense (Y0704; 5′-TATATAGGGCCCCCTCGGACCTGTCCCTGTC-3′) primers, while the sequence encoding HCV residues 364 to 715 was amplified with the same sense primer and the antisense primer Y0705 (5′-TATATAGGGCCCCCTTAATGGCCCAGGACGCG-3′). Both these PCR products were digested with *Hin*dIII and *Apa*I and ligated with pCDM8(−ApaI)+HA/CAS (HindIII-PstI), similarly digested. The resulting plasmids were designated pE2$_{661}$-HA$_{\mathrm{TMCT}}$ and pE2$_{715}$-HA$_{\mathrm{TMCT}}$. Corresponding vectors also encoding E1 sequence were generated. Primers Y0699 (5′-GCGAGCAAGCTTCCATGGGTTGCTCTTTCTCTATC-3′) and Y0704 were used in PCR with pBRTM/HCV1-3011 as the template. The product of this reaction was digested with *Hin*dIII and *Apa*I and ligated with pCDM8(−ApaI)+HA/CAS (HindIII-PstI) similarly digested to form the plasmid pE1E2$_{661}$-HA$_{\mathrm{TMCT}}$. To construct pE1E2$_{715}$-HA$_{\mathrm{TMCT}}$, pE1E2$_{661}$-HA$_{\mathrm{TMCT}}$ was digested with *Hin*dIII and *Sap*I and ligated with pE2$_{715}$-HA$_{\mathrm{TMCT}}$ similarly digested. Plasmid pE1E2, encoding the full sequence of E1 and E2, with the endogenous signal peptide, was constructed by PCR amplification with Y0699 and Y5862 (5′-GATATCCTGCAGTCACGCCTCCGCTTGGGATATGAG-3′), using pBRTM/HCV1-3011 as the template. The product of this reaction was digested with *Hin*dIII and *Pst*I and ligated with pCDM8(−ApaI) similarly digested. Plasmid pE2 was constructed by PCR of the E2 sequence with E2/FWD primer and Y5862 with pBRTM/HCV1-3011 as the template. The product of this reaction was digested with *Hin*dIII and *Pst*I. As a result of the cloning strategy described here, each recombinant chimeric protein possesses an additional Gly-Ala amino acid pair at the junction of the ectodomain (E2 sequence) and transmembrane domain (HA sequence).

Indirect immunofluorescence. HEK (293) cells were grown in DMEM supplemented with 10% FCS and 2 mM L-glutamine. Subconfluent monolayers grown in 100-mm-diameter dishes were transfected with 10 μg of plasmid by the calcium phosphate coprecipitation method. Precipitates were incubated with cells for 4 h at 37°C before being replaced with DMEM containing 2% FCS. At 48 h posttransfection, the cells were washed once with phosphate-buffered saline (PBS), fixed with 3% paraformaldehyde for 30 min at room temperature, washed with PBS, quenched with 10 mM glycine in PBS for 10 min at room temperature, washed, and permeabilized with 0.1% Triton X-100 in PBS. The permeabilization step was omitted for measurements of surface immunofluorescence. Cells were incubated with PBS containing 1% FCS and 0.05% sodium azide (P/F/A) and then incubated with primary antibodies for 1 h at room temperature. Cocktails of anti-E1 (3/8d and 3/80w) or anti-E2 (1/39, 6/82a, and 6/16) MAbs were used. After incubation with primary antibodies, the cells were washed twice with P/F/A, incubated with FITC-conjugated anti-mouse or anti-rat antibodies (at 1/500 dilution) for 1 h at room temperature, and washed three times with P/F/A. Immunofluorescence was visualized under an Axiovert 135 fluorescence microscope (Zeiss).

Expression and purification of GST-CD81EC2. The human CD81 EC2 was made from a gel-purified *Hin*cII-*Rsa*I fragment, coding for amino acids 116 to 202, of the cDNA clone and ligated to pGEX-2T (Pharmacia) which had been cut with *Eco*RI and blunted with T4 polymerase. The pGST-CD81EC2 construct was examined by sequencing to confirm the orientation and absence of mutations. SURE *Escherichia coli* (Stratagene) transformed with the plasmid was induced with 0.1 mM isopropyl-β-D-thiogalactopyranoside (IPTG) and harvested after 3 h by centrifugation, and the pellet was lysed by sonication. The GST-CD81EC2 fusion protein was recovered by affinity chromatography on glutathione-Sepharose 4B (Pharmacia). The purified fusion protein reacted with the anti-CD81 MAbs 5A6 and 1D6 when unreduced as determined by Western blotting. As noted for cellular CD81, the reduced recombinant fusion protein did not react with the antibodies (1).

Flow-cytometric analysis. HEK cells were transfected as described above. At 48 h posttransfection, the cells were harvested with PBS containing 0.2 mM EDTA and washed with PBS twice. They were incubated for 30 min at room temperature in PBS containing 1% FCS and 0.05% sodium azide (P/F/A). Viable-cell counts were determined (trypan blue exclusion), and the cells were resuspended at 10^7/ml in P/F/A. A total of 10^6 cells were incubated with 100 μl of primary antibodies (anti-E2 linear MAbs; 1/39, 6/82a, and 6/16 equal volumes of tissue-culture supernatant or anti-E2 conformational MAbs; H2, H31, H33, H44, H50, H53, H60, and H61 at 10 μg/ml, kindly supplied by J. Dubuisson, Institut Pasteur de Lille) or with 100 μl of recombinant CD81 protein, diluted in P/F/A for 1 h at room temperature. The cells were washed three times with P/F/A before addition of 100 μl of PE-conjugated secondary antibody (at 1/100 dilution). Experiments assessing the binding of GST fusion proteins to transfected cells included an additional incubation with an anti-GST MAb (100 μl of tissue-culture supernatant). After incubation for 1 h at room temperature, the cells were washed three times with P/F/A and analyzed with a FACScan apparatus. The data were processed with CellQuest software (Becton Dickinson).

Cell-cell fusion assay. HEK cells were infected with influenza A virus A/WSN/33 at a range of multiplicities of infection in serum-free DMEM for 7 h at 37°C. The virus inoculum was removed, and the cells were incubated for 1 h at 37°C with DMEM containing 1% FCS. The cells were washed free of FCS, incubated for 3 min at room temperature in PBS containing 10 mM morpholineethanesulfonic acid (MES) and 10 mM HEPES at either pH 5.0 or pH 7.0, washed with PBS, and incubated at 37°C in DMEM containing 2% FCS. Transfected cells were treated similarly. Following overnight incubation, the cells were fixed with methanol-acetone and E2 or NP antigen was visualized by indirect immunofluorescence as described above. To visualize nuclear DNA, a mountant containing propidium iodide (Vectashield; Vector Laboratories) was used. The cells were visualized with a confocal microscope (Bio-rad).

Generation and analysis of pseudotyped influenza viruses. COS-7 cells were electroporated either with empty vector, pCDM8, or with 15 μg of plasmid pE2$_{661}$-HA$_{TMCT}$ as described elsewhere (2). Following electroporation, the cells were resuspended in DMEM containing 10% FCS and 10 mM HEPES (pH 7.4) and allowed to recover at 37°C overnight. They were then infected with influenza A virus A/PR8/34 at a multiplicity of infection of 3. After 24 h, supernatants were collected and clarified of cellular debris by centrifugation at 15,000 rpm in a Beckman SW55 rotor. To confirm that the released virus contained the E2$_{661}$-HA$_{TMCT}$ protein, virus was purified by centrifugation at 45,000 rpm in a Beckman SW55 rotor through a 1-ml cushion of 30% sucrose in NTE (100 mM NaCl, 10 mM Tris-HCl [pH 7.8], 1 mM EDTA). Virus pellets were resuspended in 10 μl of NTE and subjected to sodium dodecyl sulfate-polyacrylamide gel electrophoresis (SDS-PAGE) and Western blotting to detect the incorporation of E2$_{661}$-HA$_{TMCT}$ into particles. Cell lysates were generated by lysis of transfected COS-7 cells, or MDCK cells stably expressing the A/WSN/33 M2 protein, grown to confluency in 35-mm-diameter dishes. The cells were washed once in ice-cold PBS and incubated with lysis buffer (100 mM NaCl, 50 mM iodoacetamide, 1% Nonidet P-40, 0.1% SDS, 0.5% sodium deoxycholate, 20 mM Tris HCl [pH 7.5]) on ice for 10 to 30 min. After SDS-PAGE, the E2 antigen was detected by Western blotting with rat anti-E2 MAbs followed by an anti-rat HRP-conjugated secondary antibody. The influenza A virus M2 protein was detected by using a mouse MAb, 14C2 (kindly supplied by R. A. Lamb, Northwestern University, Evanston, Ill.), followed by an anti-mouse HRP-conjugated secondary antibody. Proteins were visualized following exposure to enhanced chemiluminescence detection reagents (Amersham Life Sciences) and photographic film.

RESULTS

Truncated E2 with transmembrane and cytoplasmic domains of influenza virus HA is expressed at the cell surface. Since C-terminal truncation of E2 results in protein secretion from the cell (29, 30, 45, 47), we reasoned that addition of a transmembrane domain to such a truncated form may result in localization at the plasma membrane. To test this hypothesis, cDNA encoding the chimeric gps was constructed, consisting of the E2 ectodomain (from amino acids 384 to 661 or 715) fused to the transmembrane and cytoplasmic domains of influenza A virus HA (Fig. 1). Since the E2 gp acts as a chaperone for E1 folding (30), we were interested in determining any effects of coexpression of the full-length E1 protein on both E1 and E2 localization. Plasmids encoding both E1 and the chimeric E2 gps were therefore constructed (Fig. 1). All plasmids contained endogenous signal sequences to direct translocation to the ER, including polyprotein residues 364 to 383 for E2 chimeras and 171 to 191 for E1-encoding plasmids.

HEK (293) cells were transfected with the plasmids shown in Fig. 1, and 48 h posttransfection the cells were fixed, with or without Triton X-100 permeabilization, to monitor internal and cell surface-expressed antigen, respectively. Indirect immunofluorescence was performed with MAbs specific for both E1 and E2 proteins. The results are summarized in Table 1. As expected, full-length E1 and E2 could not be detected at the cell surface whereas E2$_{661}$-HA$_{TMCT}$ could be detected. Coexpression of E1 did not result in E1 expression at the cell surface, nor did it have any detectable effect(s) on E2$_{661}$-HA$_{TMCT}$ cell surface expression. When E2$_{715}$-HA$_{TMCT}$ was expressed, weak fluorescence could be detected both intracellularly and at the cell surface, suggesting that E2$_{715}$-HA$_{TMCT}$ was expressed less efficiently than E2$_{661}$-HA$_{TMCT}$. Similar results were obtained when E2 expression was quantified by analysis of transfected cells by flow cytometry (data not shown). The reduced expression of the E2$_{715}$-HA$_{TMCT}$ gp is consistent with previous observations about the secretion of E2, truncated at residue 715 relative to 661, and may relate to the folding efficiency of the truncated proteins (4, 26, 30).

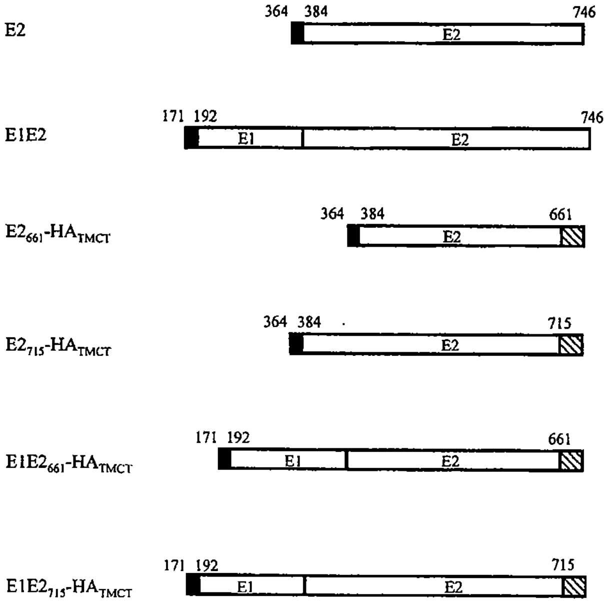

FIG. 1. Schematic representation of the proteins expressed in these studies. HCV E1 or E2 sequences were fused to the transmembrane and cytoplasmic domains of influenza A virus HA protein. The amino acid position on the HCV polyprotein is indicated above the bars. Signal sequences are indicated by solid boxes, while the HA sequence is shown by hatching. These chimeric proteins were cloned in the eukaryotic expression vector pCDM8.

Recognition of cell surface E2 by conformation-dependent anti-E2 MAbs: the effect of low-pH treatment. We were interested in determining if cell surface-expressed E2$_{661}$-HA$_{TMCT}$ was recognized by MAbs reported to specifically interact with correctly folded E2 (4, 6). HEK cells were transfected with pE2$_{661}$-HA$_{TMCT}$ and with control empty vector and at 48 h posttransfection were assayed for their ability to bind a panel of MAbs specific for linear and conformation-dependent epitopes. MAb recognition of transiently expressing cells was analyzed by flow cytometry. All of the conformation-dependent MAbs (H2, H31, H33, H44, H50, H53, H60, and H61) were able to recognize the chimeric gp, with mean fluorescence intensities in the range of 85.3 to 220.3 for E2-expressing cells stained in PBS and with background values for mock-transfected cells of 4.5 to 9.3 (data not shown and Fig. 2). These data suggest that the chimeric E2 gp is expressed in a conformation similar to that suggested for native E2 and may therefore be considered an accurate model of E2 expressed on HCV virions.

The entry of flaviviruses into cells is believed to occur by an

TABLE 1. Summary of indirect immunofluorescence observed for E1 and E2 localization on transiently expressing cells.

Plasmid	Fluorescence intensity with[a]:			
	Anti-E1		Anti-E2	
	Internal	Surface	Internal	Surface
Vector	–		–	
pE2			+++	–
pE1E2	+++	–	+++	–
pE2$_{661}$-HA$_{TMCT}$			+++	+++
pE1E2$_{661}$-HA$_{TMCT}$	+++	–	+++	+++
pE2$_{715}$-HA$_{TMCT}$			+++	++
pE1E2$_{715}$-HA$_{TMCT}$	+++	–	+++	++

[a] The intensity of fluorescence across a number of fields is indicated.

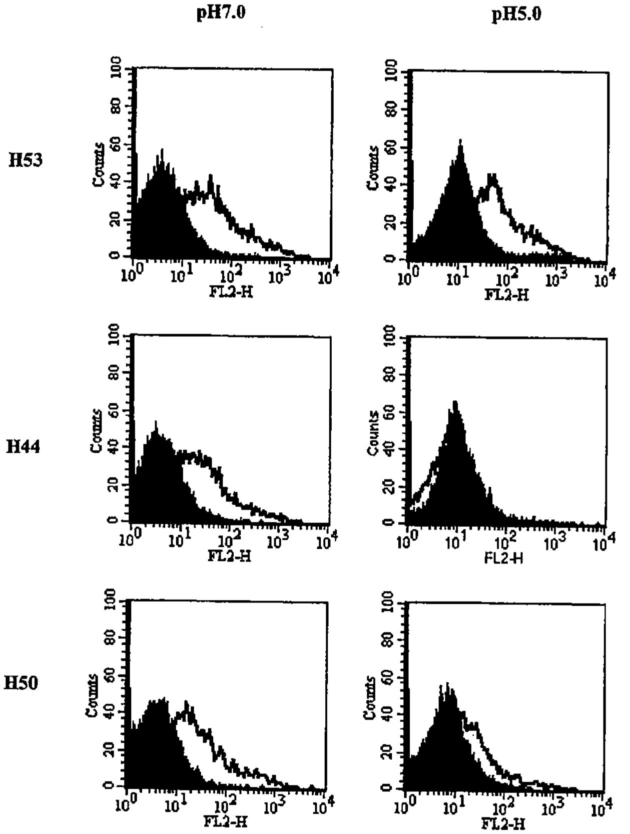

FIG. 2. Conformation of cell surface E2$_{661}$-HA$_{\mathrm{TMCT}}$. HEK cells were transfected with control empty vector (solid histograms) or with pE2$_{661}$-HA$_{\mathrm{TMCT}}$ (empty histograms). At 48 h posttransfection, cells were harvested and treated with pH 5.0 or 7.0 buffer. Cells were washed, resuspended in PBS, and immunostained with MAb H53, H44, or H50. Bound antibody was detected with PE-conjugated rabbit anti-mouse immunoglobulin antibody and flow cytometry.

acid-mediated fusion mechanism, with conformational change(s) being detectable in the envelope gp E after exposure to low pH (14, 16, 20, 40). To determine if a similar mechanism might operate for HCV, E2$_{661}$-HA$_{\mathrm{TMCT}}$-expressing cells were incubated at pH 5 or 7 for 15 min, washed twice, resuspended in PBS, and assayed for their ability to bind the conformation-dependent MAbs. As controls, MHC class I and CD81 expression were monitored and the MAbs were shown to bind equivalently independent of the pH treatment (data not shown). Most of the MAbs bound to the pH 7- or 5-treated cells equivalently, with the exception of MAbs H44 and H50 (data not shown and Fig. 2). MAb H44 failed to recognize pH 5.0-treated E2$_{661}$-HA$_{\mathrm{TMCT}}$, and recognition by H50 was reduced after pH 5.0 treatment (Fig. 2). Since the cells were resuspended in PBS after being treated at pH 5.0 or 7.0, the conformational change(s) that occurred was irreversible. Similar results were observed by enzyme-linked immunosorbent assay for MAb recognition of low-pH-treated soluble E2$_{661}$ gp (data not shown). These data are consistent with reports regarding the sensitivity of the flavivirus gp E to low pH treatment.

E2$_{661}$-HA$_{\mathrm{TMCT}}$ binds recombinant CD81, a putative receptor for HCV. Recently, CD81 has been identified as a putative receptor for HCV (36). Binding of E2 to cells may be blocked by a recombinant fusion protein containing the second extracellular loop (EC2) of CD81 (9, 36). It was of interest, therefore, to determine if cell surface-expressed E2$_{661}$-HA$_{\mathrm{TMCT}}$ could bind a recombinant form of CD81, GST-CD81 containing the EC2. This GST-CD81EC2 protein is able to bind a number of conformation-dependent CD81 specific MAbs and to inhibit the interaction of soluble E2 with CD81-positive cells (9). HEK cells were transfected with either pE2$_{661}$-HA$_{\mathrm{TMCT}}$ or empty vector and at 48 h posttransfection were monitored for both E2 expression and the ability to bind GST-CD81EC2 and a control protein, GST-nef. FACScan analysis demonstrated that 25% of the cells expressed E2 at their surface (Fig. 3A) and that a percentage of these cells were able to bind GST-CD81EC2. No significant binding of GST-nef to cells transfected with vector or with pE2$_{661}$-HA$_{\mathrm{TMCT}}$ was detected. When GST-CD81EC2 (20 μg/ml) was incubated with mock-transfected cells, a low-level binding was observed (2.1% positive cells); however, a higher level of GST-CD81EC2 cell binding was detected for cells expressing E2$_{661}$-HA$_{\mathrm{TMCT}}$, i.e., 10.8% (Fig. 3B). Similar results were observed with a reduced concentration of GST-CD81EC2 (5 μg/ml). These figures are lower than the percentage of cells expressing E2$_{661}$-HA$_{\mathrm{TMCT}}$ on their surface, possibly because GST-CD81EC2 binding was not saturated or because the affinity of the anti-GST MAb for the cell-bound GST-CD81EC2 was lower than that of the anti-E2 MAbs for E2. However, we cannot exclude the possibility that the EC1 loop of CD81 (lacking from this recombinant fusion protein) influences the affinity of EC2 for E2. These data confirm that cell surface-expressed chimeric E2 can bind a recombinant form of CD81, with the binding site residing between residues 384 and 661, and that E2$_{661}$-HA$_{\mathrm{TMCT}}$ is active in the (putative) receptor-binding function.

E2 at the cell surface does not induce acid-mediated cell-cell fusion. Fusion of cells expressing influenza virus HA protein by acid treatment has been well characterized (reviewed in references 11, 17, and 50). Since flaviviruses have been reported to enter cells via receptor-mediated endocytosis, we were interested in determining if E2$_{661}$-HA$_{\mathrm{TMCT}}$ could induce cell-cell fusion in CD81-positive cells after acid treatment. HEK and the glial cell line, U87, were shown to express CD81 with mean fluorescence intensities of 958.4 and 120.3, respectively, by using the CD81-specific MAb 5A6, whereas an irrelevant isotype-matched control MAb gave values of 8.9 and 12.3 (data not shown). HEK cells transiently expressing E2$_{661}$-HA$_{\mathrm{TMCT}}$ were treated at pH 5.0 or 7.0 as detailed above and incubated at 37°C overnight. E2-expressing cells were detected by indirect immunofluorescence, using MAbs 1/39, 6/82, and 6/16, and the nuclei were visualized with propidium iodide. After neutral- or low-pH treatment, no cell-cell fusion of cells expressing E2 at their surface was observed (Fig. 4C). As a positive control for the assay, HEK cells were infected with influenza A virus strain A/WSN/33 at different multiplicities of infection. This strain was chosen because cleavage of HA$_0$ to HA$_1$ and HA$_2$, a necessary prelude to fusion, does not require trypsin treatment. Influenza virus-infected cells were identified by using an antibody specific for nucleoprotein (NP). Influenza virus-mediated cell fusion was easily detected, with large syncytia forming around NP-positive cells following low-pH treatment (Fig. 4B) but not after neutral-pH treatment (Fig. 4A). The syncytia were most evident at high multiplicities of infection, in line with previous observations that membrane fusion may be dependent upon the local density of fusion protein (5). However, the U87 glial cell line is a more sensitive indicator cell for studying both influenza virus- and human immunodeficiency virus-mediated cell fusion (24); hence, the experiment detailed above with E2$_{661}$-HA$_{\mathrm{TMCT}}$ was repeated in this cell line. Comparable results were obtained, such that no E2$_{661}$-HA$_{\mathrm{TMCT}}$-mediated cell fusion was observed; however, influenza virus-

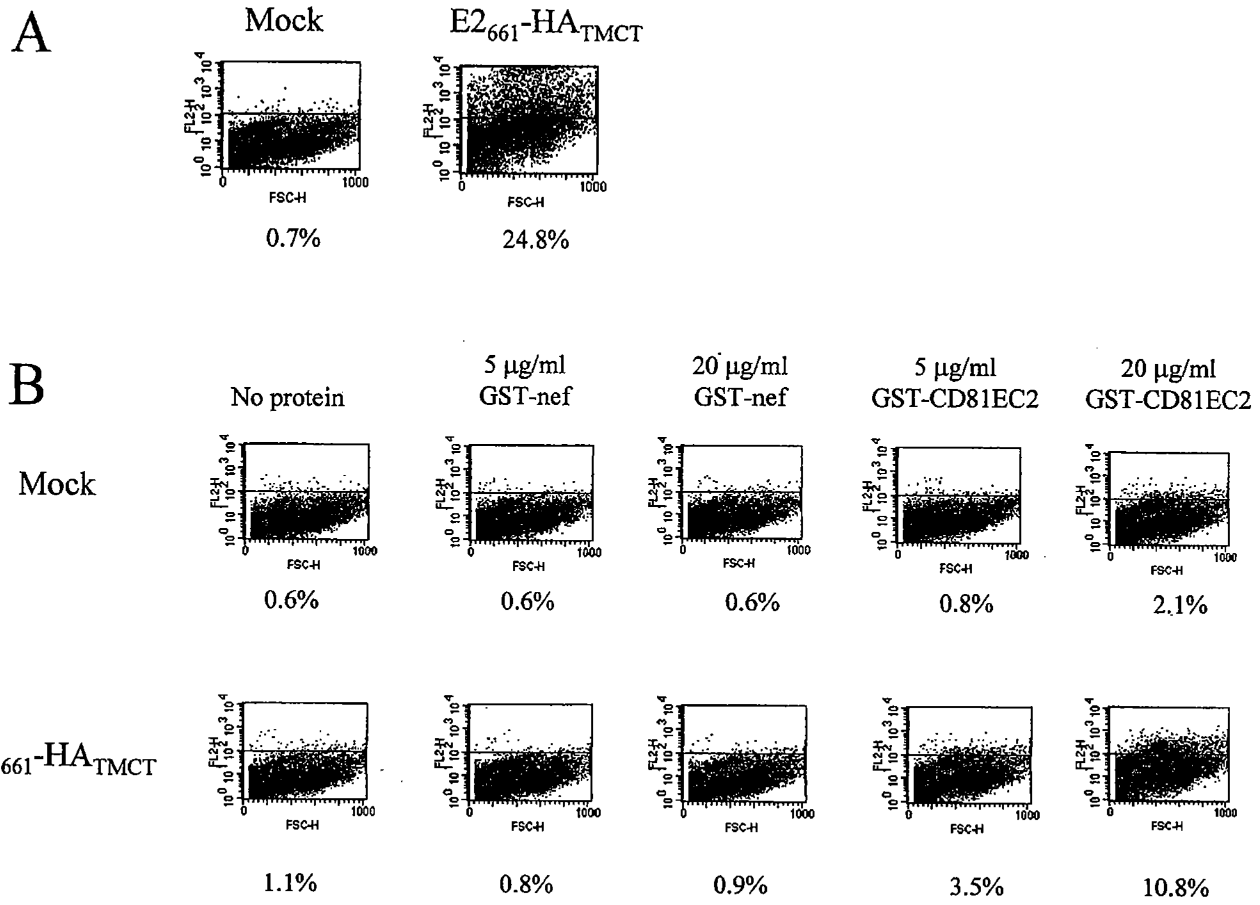

FIG. 3. E2$_{661}$-HA$_{TMCT}$ binds recombinant CD81. (A) Expression of E2$_{661}$-HA$_{TMCT}$ on transfected HEK (293) cells. Cells were transfected with pE2$_{661}$-HA$_{TMCT}$ or with control empty vector. At 48 h posttransfection, the cells were immunostained with rat anti-E2 antibodies followed by PE-conjugated rabbit anti-rat immunoglobulin and were subjected to flow cytometric analysis. The results are presented as dot plots of forward scatter (FSC) against PE fluorescence in the FL2 channel. The percentage of E2-positive cells is indicated. (B) Binding of GST-CD81EC2 to E2$_{661}$-HA$_{TMCT}$-expressing cells. HEK (293) cells were transfected with control empty vector or with pE2$_{661}$-HA$_{TMCT}$. At 48 h posttransfection, the cells were incubated with no GST fusion protein, GST-nef, or GST-CD81EC2 at the concentrations indicated. Bound GST fusion protein was detected with a rat anti-GST MAb (2/18) followed by a PE-conjugated rabbit anti-rat immunoglobulin antibody. The percentage of positive cells is indicated below each plot.

induced fusion was observed at all multiplicities of infection tested (data not shown). These data indicate that under conditions which support cell-cell fusion by the influenza virus HA protein, the chimeric E2$_{661}$-HA$_{TMCT}$ gp does not induce any detectable cell fusion.

E2$_{661}$-HA$_{TMCT}$ can be incorporated into influenza virus particles. Influenza A viruses do not incorporate significant levels of host cell proteins into their envelopes. However, possession of HA transmembrane and cytoplasmic tail sequences has previously been shown to direct the incorporation of foreign proteins into influenza virus particles (31, 52). Since E2$_{661}$-HA$_{TMCT}$ was expressed at the cell surface and contained the relevant HA sequences, we tested the ability of influenza A virus to incorporate the chimeric gp expressed in COS cells. It is important to note that we (9) and others (36) have previously shown that E2 is unable to bind to COS-expressed CD81, such that high level expression of E2$_{661}$-HA$_{TMCT}$ can be achieved without receptor ligand complex formation. COS-7 cells were electroporated with pE2$_{661}$-HA$_{TMCT}$ (Fig. 5A and B, lanes 2 and 4) or empty vector (lanes 1 and 3). Cells were infected with influenza virus 24 h after transfection (multiplicity of infection, 3; lanes 1 and 2), and the extracellular progeny virus was harvested after a further 24 h. Virions were separated from host cell membrane fragments by ultracentrifugation through a high-density sucrose cushion and characterized for their constituent proteins by Western blotting. The influenza virus protein M2, a minor component of influenza virus, was visible, confirming the presence of influenza A virus particles derived from infected cells (Fig. 5B). E2 antigen was detected in a lysate derived from pE2$_{661}$-HA$_{TMCT}$-transfected cells (Fig. 5A, lane 4), indicating that expression had occurred in these cells. Furthermore, this protein was incorporated into influenza virus particles, since it was present in progeny virions from cells transfected with pE2$_{661}$-HA$_{TMCT}$ (Fig. 5A, lane 2). The E2$_{661}$-HA$_{TMCT}$ in a lysate of expressing cells and that incorporated into influenza virus virions was compared (Fig. 5C). Since influenza virus virions bud through the plasma membrane, the chimeric molecule would be expected to undergo modification with complex glycans during transport through the secretory transport system. Consistent with this, the E2$_{661}$-HA$_{TMCT}$ present in a lysate from expressing cells migrated more rapidly in SDS-PAGE (Fig. 5C, lane 1) than did that present in influenza virus virions (lane 2).

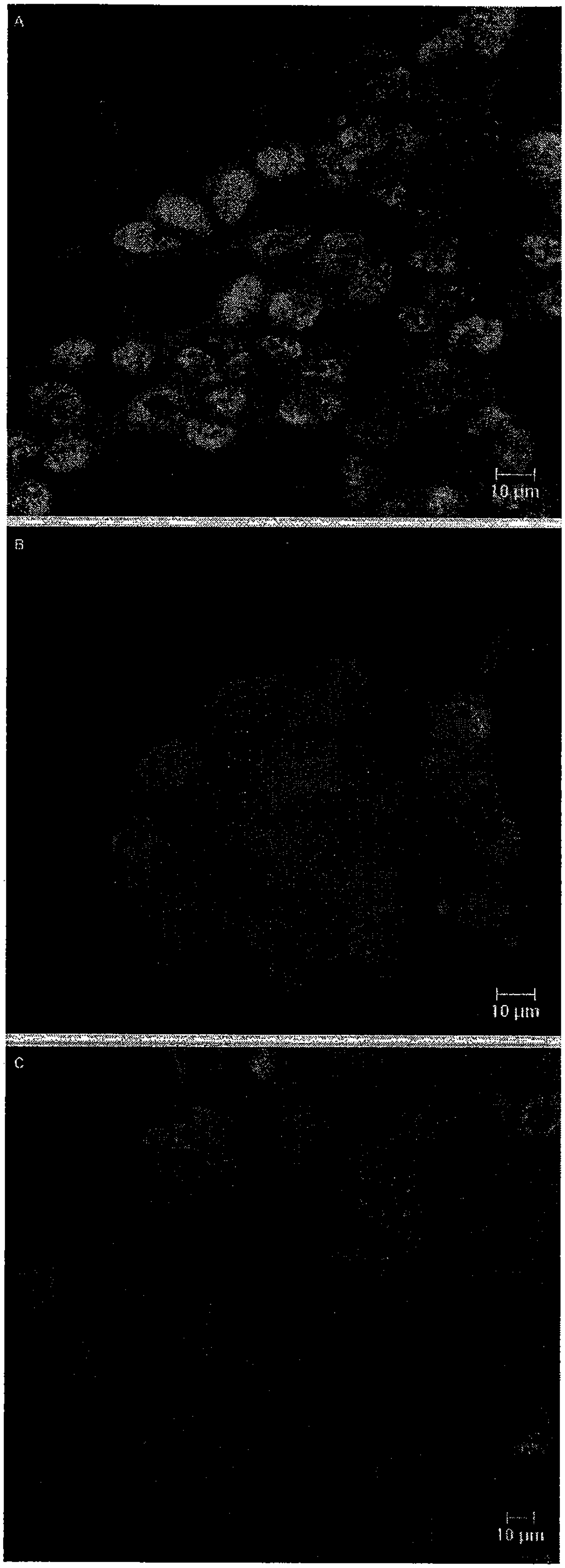

FIG. 4. Cell-cell fusion is not mediated by $E2_{661}$-HA_{TMCT} under conditions which permit HA-mediated fusion. HEK cells were infected with influenza A virus (A and B) or transfected with plasmid $pE2_{661}$-HA_{TMCT} (C). Cell monolayers were treated at pH5.0 (B and C) or pH 7.0 (A) and visualized by indirect immunofluorescence with anti-E2 antibodies for transfected cells, or anti-NP MAb for influenza virus-infected cells, with propidium iodide to visualize nuclei. These micrographs show representative fields from the examined samples.

DISCUSSION

The current understanding of HCV gp function is limited by the lack of a tissue culture system supporting efficient replication of the virus. From studies with transient-expression systems, it is believed that gps E1 and E2 localize to the ER in infected cells (4, 6, 8). By analogy to other flaviviruses, virus morphogenesis may involve budding into the ER and subsequent transport of viral particles through the host cell secretory pathway before release into the extracellular space. Modification of flavivirus E and prM protein glycans by trimming and terminal addition suggests that virions do indeed move through an exocytosis pathway similar to that used for host gps (27, 32).

In this report we describe a truncated form of the HCV E2 gp fused to the transmembrane and cytoplasmic domains of the influenza A virus HA protein. This chimeric protein was expressed at the cell surface, where it was able to bind a number of conformation-dependent MAbs and a recombinant soluble version of the putative HCV receptor, CD81 (Table 1; Fig. 2 and 4). These data suggest that the chimeric gp is folded in a manner comparable to E2 present in native E1E2 complexes and that it is in a form able to bind the putative receptor, CD81. Low-pH treatment of cell surface-expressed E2 resulted in a conformational change(s). However, neutral- or low-pH treatment of CD81-positive cells expressing the chimeric gp at the cell surface did not result in cell fusion.

If HCV virions are indeed transported through the host cell secretory pathway, then $E2_{661}$-HA_{TMCT} should resemble E2 on the surface of virions. Understanding the way in which E2 is glycosylated may help our understanding of E2 conformation and structure. Inhibition of core glycosylation by tunicamycin prevents E2 from folding correctly and being recognized by the conformation-dependent MAbs (1a). Since $E2_{661}$-HA_{TMCT} reacts with such MAbs and since H2 and H53 react with noncovalently associated E1E2 heterodimers (4, 6), this indicates that $E2_{661}$-HA_{TMCT} has a conformation similar to that adopted in E1E2 complexes.

A proteolytic cleavage is a common posttranslational modification of viral membrane proteins (reviewed in reference 21). For example, during virion transit, the prM protein of flaviviruses is cleaved by the host protease furin within a post-Golgi acidic compartment (15, 38, 48). This cleavage is required for the acquisition of virion infectivity. No proteolytic cleavage was detectable in deglycosylated $E2_{661}$-HA_{TMCT}, since no size differences were observed when expressing cells were treated with or without brefeldin A, an inhibitor of the secretory transport system (data not shown). This suggests that, unlike prM, HCV E2 does not undergo proteolytic cleavage as a step in virus maturation.

Previous work has shown that truncation of E2 to residue 661 results in a molecule that is more readily exported from the cell than is a molecule truncated at residue 715 (4, 26, 30). The additional residues could reduce the efficiency of E2 folding and hence of secretory transport. Our data is consistent with this hypothesis, since $E2_{661}$-HA_{TMCT} was detected more readily on the surface of expressing cells than was $E2_{715}$-HA_{TMCT} (Table 1). Given the reported chaperone role of E2 in E1 folding, we were interested in determining whether

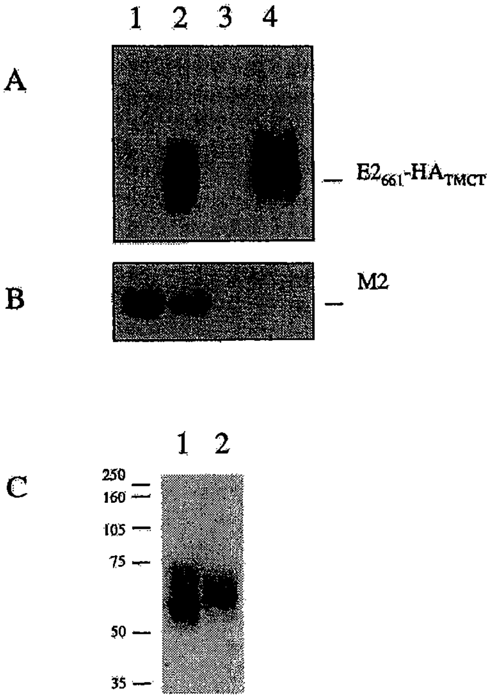

FIG. 5. Incorporation of E2$_{661}$-HA$_{\mathrm{TMCT}}$ into influenza virus particles. COS-7 cells were either mock transfected or transfected with pE2$_{661}$-HA$_{\mathrm{TMCT}}$ and infected at 24 h posttransfection with A/PR/8/34. Virus was harvested and purified 24 h postinfection and analyzed by SDS-PAGE (15% polyacrylamide) and immunoblotting for incorporation of the chimeric protein into particles. (A) Immunoblotting for the presence of E2$_{661}$-HA$_{\mathrm{TMCT}}$ with anti-E2 antibodies. Lanes 1 and 2 are purified progeny virus released from mock-transfected cells (lane 1) and cells transfected with pE2$_{661}$-HA$_{\mathrm{TMCT}}$ (lane 2). Lanes 3 and 4 are cell lysates prepared from mock-transfected COS-7 cells (lane 3) and COS-7 cells transfected with pE2$_{661}$-HA$_{\mathrm{TMCT}}$ (lane 4). (B) To confirm the presence of influenza A virus particles, the same samples were analyzed by SDS-PAGE and immunoblotting to detect M2, using the 14C2 MAb. (C) E2$_{661}$-HA$_{\mathrm{TMCT}}$ derived from a lysate of expressing cells (lane 1) and that incorporated into influenza virus virions (lane 2) was compared by SDS-PAGE (10% polyacrylamide) followed by immunoblotting with anti-E2 antibodies.

cell surface expression of E2$_{661}$-HA$_{\mathrm{TMCT}}$ would lead to expression of E1 at the cell surface (30). However, E1 was not detected at the cell surface under any circumstances; furthermore, E1 coexpression did not affect the level of E2 transport to the plasma membrane.

It is thought that after receptor-mediated endocytosis, flavivirus entry into target cells proceeds via an acid-mediated fusion event, where the viral envelope fuses with an endosomal membrane. Acid treatment of the flavivirus envelope protein E in mature virions results in a conformational change (14, 16, 20, 40). This conformational change is irreversible and results in the exposure of new antigenic epitopes and the loss of others. Treatment of cell surface-expressed E2$_{661}$-HA$_{\mathrm{TMCT}}$ with pH 5.0 buffer caused an irreversible conformational change recognized by MAbs H44 and H50 (Fig. 2). These data suggest that HCV may enter target cells via a mechanism similar to that used by other flaviviruses. However, it should be noted that changes in E2$_{661}$-HA$_{\mathrm{TMCT}}$ conformation after pH 5.0 treatment may be unrelated to an acid-mediated mode of entry.

We were unable to demonstrate any E2$_{661}$-HA$_{\mathrm{TMCT}}$-mediated cell-cell fusion (Fig. 4 and data not shown). However, the conditions used in this assay, although compatible with influenza virus HA-mediated fusion, might not support E2-mediated fusion. The production of polykaryotic cells is dependent upon the density of the fusion protein at the cell surface (5), and the expression method used may not result in a sufficient accumulation of cell surface E2$_{661}$-HA$_{\mathrm{TMCT}}$ to support fusion. Alternatively, the lipid composition of HEK and U87 cell membranes may not be compatible with E2-mediated fusion (12, 49). In any event, the lack of detectable polykaryons is not definitive evidence that HCV E2 does not have a fusogenic activity, since variant influenza viruses, herpesviruses, and paramyxoviruses exist that do not cause syncytium formation even though they are active in their fusion function (50). Another explanation is that E1 is required, or indeed is responsible, for the fusion event. Since we were unable to demonstrate any fusion activity for E2$_{661}$-HA$_{\mathrm{TMCT}}$, we examined the sequence of E1 for a putative fusion peptide. Interestingly, recombinant E1 protein is secreted when truncated after amino acid 340, only if an internal deletion between residues 262 and 290 is also present (29). This internal deletion spans a hydrophobic domain, possibly containing a fusion peptide, that could act as a transmembrane anchor when E1 is truncated at residue 340, preventing its secretion. Viral fusion peptides may act as transmembrane anchor domains, converting normally soluble proteins into membrane-bound ones (34). Most fusion peptides are composed of 16 to 26 relatively hydrophobic amino acids (50). The sequence of the internal hydrophobic domain in E1 is relatively highly conserved, with changes usually being conservative (Fig. 6A) (25). Alignment of this region of HCV E1 with the putative fusion peptide from flavivirus E proteins (41) revealed several similarities (Fig. 6B). Two Cys residues are completely conserved between all sequences analyzed. The structural implications of this are unclear, but if these residues were involved in disulfide bonds, the putative fusion peptide may be constrained in some fashion. An Asp residue is present in all the representative HCV sequences and some of the flavivirus sequences. The presence of acidic residues in the fusion peptides of some low-pH-activated viral fusion proteins has been noted previously (51). Two Gly residues are conserved within these putative fusion domains. The Gly residues within the E1 sequences have a spacing similar to that observed in the fusion peptides of the paramyxoviruses, at positions 3, 7, and 12 and at positions 3, 7, and 13 for the majority of HCV sequences analyzed to date (Fig. 6C). In the paramyxovirus F proteins, the Gly residues are believed to be important for the structure of the fusion peptide (19). Given the similarities between the internal hydrophobic region of HCV E1, the putative (flavivirus) and known (paramyxovirus) fusion peptides, we propose that this region may comprise the HCV fusion peptide.

Some enveloped viruses are promiscuous in regard to the proteins they will incorporate into their membrane, while others appear to use specific signals in the sequences of their envelope proteins to discriminate between viral and cellular proteins present at the site of budding. Influenza virus appears to utilize transmembrane and cytoplasmic tail sequences to select its major envelope protein, HA, during particle formation (31). Hence, it is not surprising that E2 expressing the HA$_{\mathrm{TMCT}}$ was incorporated efficiently into influenza virus particles (Fig. 5). In contrast, VSV has the capacity to incorporate foreign gps regardless of their amino acid sequence (44) and has been used extensively to study many viral gps. VSV particles expressing either chimeric HCV E1 or E2 gps were recently reported to confer VSV entry, suggesting that the gps could function independently to mediate binding and entry into target cells (22). The entry of these pseudotyped viruses could be inhibited by sera from chimpanzees immunized with the homologous HCV gps; however, the entry was not shown

A

```
        264                          290
1a    : LLVGSATLCSALYVGDLCGSVFLVGQLFTF :
1b    : ....A.A....M............S..... :
2a    : MV.M...............G.M.AA.M.IV :
2b    : MI.MA..A........V..A.MILS.A.MV :
3a    : ....A..M........M..A......A... :
4a    : .M..A..V..V........GA.....M... :
5a    : Y.A.G.A.........A..AL.....M..Y :
6a    : ..A.A.VV..S..I......L..A...... :
7d    : ....A.AF...M.......GL......... :
8a    : ......A......I.....G.......... :
9a    : ....A.AF...M.I......II........ :
10a   : MM..A..............AL.....G.SW :
11a   : .M..A.A....M.L.....G.......... :
```

B

```
              265                    287
HCV-1a      : LVGSATLCSALYVG--DLCGSVFLV :
TBE         : DRGWGNHCGLFGKGSIVACVKAA-  :
YF          : DRGWGNGCGLFGKGSIVACAKFT-  :
JE          : DRGWGNGCGLFGKGSIDTCAKFS-  :
DEN1        : DRGWGNGCGLFGKGSLITCAKFK-  :
DEN2        : DRGWGNGCGLFGKGGIVTCAMFT-  :
DEN4        : DRGWGNGCGLFGKGGVVTCAKFS-  :
KUN         : DRGWGNGCGLFGKGSIDTCAKFA-  :
WNE         : DRGWGNGCGLFGKGSIDTCAKFA-  :
MVE         : DRGWGNGCGLFGKGSIDTCAKFT-  :
SLE         : DRGWGNGCGLFGKGSIDTCAKFT-  :
```

C

```
              275            293
HCV-1a      : YVGDLCGSVFLVGQLFTF-- :
HPIV1       : FFGAVIGTIALGVATAAQIT :
HPIV2       : FAGVVVGLAALGVATAAQIT :
HPIV3       : FFGGVIGTIALGVATSAQIT :
MEASLES     : FAGVVLAGAALGVATAAQIT :
CDV         : FAGVVLAGAALGVATAAQIT :
RINDERPEST  : FAGVALAGAALGVATAAQIT :
SV5         : FAGVVIGLAALGVATAAQVT :
SV41        : FAGVVVGLAALGVATAAQIT :
MUMPS       : FAGIAIGIAALGVATAAQVT :
SENDAI      : FFGAVIGTIALGVATSAQIT :
NDV         : FIGAIIGSVALGVATAAQIT :
```

FIG. 6. A putative fusion peptide within the E1 protein. Numbers above the alignments indicate the amino acid position within the HCV-1 polyprotein. (A) Alignment of the internal hydrophobic domain of representative HCV genotypes (25). (B) The HCV putative fusion peptide contains similarities to the predicted fusion peptide from flavivirus E glycoprotein. Shown are alignments of the HCV-1 sequence with representative flavivirus fusion peptides: YF, yellow fever virus; JE, Japanese encephalitis virus; DEN, Dengue virus; KUN, Kunjin virus; WNE, West Nile virus; MVE, Murray Valley encephalitis virus; SLE, St. Louis encephalitis virus (41). Residues completely conserved across these sequences are shaded. (C) Spacing of Gly residues within the HCV putative fusion peptide is similar to that within the fusion peptides of paramyxovirus F proteins. Alignment of the HCV-1 sequence with representative paramyxovirus fusion peptide sequences: HPIV, human parainfluenza virus; SV, simian virus; CDV, canine distemper virus; NDV, Newcastle disease virus (19). Gly residues are shaded.

to be CD81 dependent. Clearly, it will be important to demonstrate whether CD81, either alone or with additional factors, can function as the HCV receptor in allowing pseudotyped virus-cell attachment and entry. Since CD81 is so widely expressed, it is unlikely to be the sole factor determining HCV liver tropism. We are now in an ideal position to answer these questions by studying the receptor requirements for attachment, entry, and uncoating of influenza viruses expressing chimeric HCV gps.

ACKNOWLEDGMENTS

We thank D. Steinhauer for the HA clone, J. Dubuisson for conformation-dependent MAbs specific for HCV E2, R. A. Lamb for antibodies specific for influenza virus proteins, and M. Harris for GST-nef. We are also indebted to Yasmin Chaudhry, Barbara Konig, Moy Robson, and Stephen Poutney for excellent technical assistance. We thank Peter Balfe and Jeff Almond for constructive comments on the manuscript.

The work described herein was supported by The Wellcome Trust and The University of Reading Research Endowment Trust and by Public Health Service grant CA 34233 from the National Institutes of Health (to S.L.). J.M.T. received support through a BBSRC special studentship.

REFERENCES

1. **Andria, M. L., and S. Levy.** Unpublished results.
1a. **Choukhi, A., S. Ung, C. Wychowski, and J. Dubuisson.** 1998. Involvement of endoplasmic reticulum chaperones in the folding of hepatitis C virus glycoproteins. J. Virol. **72:**3851–3858.
2. **Chu, G., H. Hayakawa, and P. Berg.** 1987. Electroporation for the efficient transfection of mammalian cells with DNA. Nucleic Acids Res. **15:**1311–1326.
3. **Clarke, B.** 1997. Molecular virology of hepatitis C virus. J. Gen. Virol. **78:**2397–2410.
4. **Cocquerel, L., J.-C. Meunier, A. Pillez, C. Wychowski, and J. Dubuisson.** 1998. A retention signal necessary and sufficient for endoplasmic reticulum localization maps to the transmembrane domain of hepatitis C virus glycoprotein E2. J. Virol. **72:**2183–2191.
5. **Danieli, T., S. L. Pelletier, Y. I. Henis, and J. M. White.** 1996. Membrane fusion mediated by the influenza hemagglutinin requires the concerted action of at least three hemagglutinin trimers. J. Cell Biol. **133:**559–569.
6. **Deleersnyder, V., A. Pillez, C. Wychowski, K. Blight, J. Xu, Y. S. Hahn, C. M. Rice, and J. Dubuisson.** 1997. Formation of native hepatitis C virus glycoprotein complexes. J. Virol. **71:**697–704.
7. **Dubuisson, J.** Folding, assembly and subcellular localization of HCV glycoproteins. Curr. Top. Microbiol. Immunol., in press.
8. **Dubuisson, J., H. H. Hsu, R. C. Cheung, H. B. Greenberg, D. G. Russell, and C. M. Rice.** 1994. Formation and intracellular localization of hepatitis C virus envelope glycoprotein complexes expressed by recombinant vaccinia and Sindbis viruses. J. Virol. **68:**6147–6160.
9. **Flint, M., C. M. Maidens, L. Loomis-Price, C. Shotton, J. Dubuisson, P. Monk, A. Higginbottom, S. Levy, and J. A. McKeating.** 1999. Characterization of hepatitis C virus E2 glycoprotein interaction with a putative cellular receptor, CD81. J. Virol. **73:**6235–6244.
10. **Flint, M., and J. A. McKeating.** The C-terminal region of the hepatitis C virus E1 glycoprotein confers localisation within the endoplasmic reticulum. J. Gen. Virol., in press.
11. **Gaudin, Y., R. W. H. Ruigrok, and J. Brunner.** 1995. Low-pH induced conformational changes in viral fusion proteins: implications for the fusion mechanism. J. Gen. Virol. **76:**1541–1556.
12. **Gollins, S. W., and J. S. Porterfield.** 1986. pH-dependent fusion between the flavivirus West Nile and liposomal model membranes. J. Gen. Virol. **67:**157–166.
13. **Grakoui, A., C. Wychowski, C. Lin, S. M. Feinstone, and C. M. Rice.** 1993. Expression and identification of hepatitis C virus polyprotein cleavage products. J. Virol. **67:**1385–1395.
14. **Guirakhoo, F., R. A. Bolin, and J. T. Roehrig.** 1992. The Murray Valley encephalitis virus prM protein confers acid resistance to virus particles and alters the expression of epitopes within the R2 domain of E glycoprotein. Virology **191:**921–931.
15. **Guirakhoo, F., F. X. Heinz, C. W. Mandl, H. Holzmann, and C. Kunz.** 1991. Fusion activity of flaviviruses: comparison of mature and immature (prM-containing) tick-borne encephalitis virions. J. Gen. Virol. **72:**1323–1329.
16. **Guirakhoo, F., F. X. Heinz, and C. Kunz.** 1989. Epitope model of tick-borne encephalitis virus envelope glycoprotein E: analysis of structural properties, role of carbohydrate side chain, and conformational changes occurring at acidic pH. Virology **169:**90–99.
17. **Hernandez, L. D., L. R. Hoffman, T. G. Wolfsberg, and J. M. White.** 1996. Virus-cell and cell-cell fusion. Annu. Rev. Cell Dev. Biol. **12:**627–661.
18. **Hijikata, M., N. Kato, Y. Ootsuyama, M. Nakagawa, and K. Shimotohno.** 1991. Gene mapping of the putative structural region of the hepatitis C virus genome by *in vitro* processing analysis. Proc. Natl. Acad. Sci. USA **88:**5547–5551.
19. **Horvath, C. M., and R. A. Lamb.** 1992. Studies on the fusion peptide of a paramyxovirus fusion glycoprotein: roles of conserved residues in cell fusion. J. Virol. **66:**2443–2455.

20. **Kimura, T., and A. Ohyama.** 1988. Association between the pH-dependent conformational change of West Nile flavivirus E protein and virus-mediated membrane fusion. J. Gen. Virol. **69:**1247–1254.
21. **Klenk, H.-D., and W. Garten.** 1994. Activation cleavage of viral spike proteins by host proteases, p. 241–280. *In* E. Wimmer (ed.), Cellular receptors for animal viruses. Cold Spring Harbor Laboratory Press, Cold Spring Harbor, N.Y.
22. **Lagging, L. M., K. Meyer, R. J. Owens, and R. Ray.** 1998. Functional role of hepatitis C virus chimeric glycoproteins in the infectivity of pseudotyped virus. J. Virol. **72:**3539–3546.
23. **Levy, S., S. C. Todd, and H. T. Maecker.** 1998. CD81 (TAPA-1): a molecule involved in signal transduction and cell adhesion in the immune system. Annu. Rev. Immunol. **16:**89–109.
24. **Lewis, J., P. Balfe, C. Arnold, S. Kaye, R. S. Tedder, and J. A. McKeating.** 1998. Development of a neutralizing antibody response during acute primary human immunodeficiency virus type 1 infection and emergence of antigenic variants. J. Virol. **72:**8943–8951.
25. **Maertens, G., and L. Stuyver.** 1997. Genotypes and genetic variation of hepatitis C virus, p. 183–223. *In* T. J. Harrison & A. J. Zuckerman (eds.) The molecular medicine of viral hepatitis. John Wiley & Sons Ltd., Chichester, United Kingdom.
26. **Maidens, C., C. Shotton, M. Flint, J. Dubuisson, J. W. Almond, and J. A. McKeating.** 1998. Full length and truncated forms of the HCV E2 glycoprotein differ in both their antigenic conformation and in their ability to recognise their putative cellular receptors, abstr. O032. *In* Abstracts of the 5th International Meeting of Hepatitis C virus and Related Viruses, Molecular Virology and Pathogenesis 1998.
27. **Mason, P. W.** 1989. Maturation of Japanese encephalitis virus glycoproteins produced by infected mammalian and mosquito cells. Virology **169:**354–364.
28. **Matsuura, Y., K. Ishii, H. Aizaki, S. Takigawa, H. Tani, M. A. Whitt, and T. Miyamura.** 1998. Characterization of pseudotype VSV possessing HCV envelope proteins, abstr. O006. *In* Abstracts of the 5th International Meeting of Hepatitis C Virus and Related Viruses, Molecular Virology and Pathogenesis 1998.
29. **Matsuura, Y., T. Suzuki, R. Suzuki, M. Sato, H. Aizaki, I. Saito, and T. Miyamura.** 1994. Processing of E1 and E2 glycoproteins of hepatitis C virus expressed in mammalian and insect cells. Virology **205:**141–150.
30. **Michalak, J.-P., C. Wychowski, A. Choukhi, J.-C. Meunier, S. Ung, C. M. Rice, and J. Dubuisson.** 1997. Characterization of truncated forms of hepatitis C virus glycoproteins. J. Gen. Virol. **78:**2299–2306.
31. **Naim, H. Y., and M. G. Roth.** 1993. Basis for selective incorporation of glycoproteins into the influenza virus envelope. J. Virol. **67:**4831–4841.
32. **Nowak, T., P. M. Farber, G. Wengler, and G. Wengler.** 1989. Analyses of the terminal sequences of West Nile virus structural proteins and of the *in vitro* translation of these proteins allow the proposal of a complete scheme of the proteolytic cleavages involved in their synthesis. Virology **169:**365–376.
33. **Oren, R., S. Takahashi, C. Doss, R. Levy, and S. Levy.** 1990. TAPA-1, the target of an antiproliferative antibody, defines a new family of transmembrane proteins. Mol. Cell. Biol. **10:**4007–4015.
34. **Paterson, R. G., and R. A. Lamb.** 1987. Ability of the hydrophobic fusion-related external domain of a paramyxovirus F protein to act as a membrane anchor. Cell **48:**441–452.
35. **Pettersson, R. F.** 1991. Protein localization and virus assembly at intracellular membranes. Curr. Top. Microbiol. Immunol. **170:**67–106.
36. **Pileri, P., Y. Uematsu, S. Campagnoli, G. Galli, F. Falugi, R. Petracca, A. J. Weiner, M. Houghton, D. Rosa, G. Grandi, and S. Abrignani.** 1998. Binding of hepatitis C virus to CD81. Science **282:**938–941.
37. **Ralston, R., K. Thudium, K. Berger, C. Kuo, B. Gervase, J. Hall, M. Selby, G. Kuo, M. Houghton, and Q.-L. Choo.** 1993. Characterization of hepatitis C virus envelope glycoprotein complexes expressed by recombinant vaccinia viruses. J. Virol. **67:**6753–6761.
38. **Randolph, V. B., G. Winkler, and V. Stollar.** 1990. Acidotropic amines inhibit proteolytic processing of flavivirus prM protein. Virology **174:**450–458.
39. **Rice, C. M.** 1996. *Flaviviridae*: the viruses and their replication, p. 931–959. *In* B. N. Fields, D. M. Knipe, P. M. Howley, R. M. Chanock, J. L. Melnick, T. P. Monath, B. Roizman and S. E. Straus (ed.), Fields virology, 3rd ed. Lippincott-Raven, Philadelphia, Pa.
40. **Roehrig, J. T., A. J. Johnson, A. R. Hunt, R. A. Bolin, and M. C. Chu.** 1990. Antibodies to Dengue 2 virus E-glycoprotein synthetic peptides identify antigenic conformation. Virology **177:**668–675.
41. **Roehrig, J. T., A. R. Hunt, A. J. Johnson, and R. A. Hawkes.** 1989. Synthetic peptides derived from the deduced amino acid sequence of the E-glycoprotein of Murray valley encephalitis virus elicit antiviral antibody. Virology **171:**49–60.
42. **Rosa, D., S. Campagnoli, C. Moretto, E. Guenzi, L. Cousens, M. Chin, C. Dong, A. J. Weiner, J. Y. N. Lau, Q.-L. Choo, D. Chien, P. Pileri, M. Houghton, and S. Abrignani.** 1996. A quantitative test to estimate neutralizing antibodies to the hepatitis C virus: cytofluorimetric assessment of envelope glycoprotein 2 binding to target cells. Proc. Natl. Acad. Sci. USA **93:**1759–1763.
43. **Santolini, E., G. Migliaccio, and N. L. Monica.** 1994. Biosynthesis and biochemical properties of the hepatitis C virus core protein. J. Virol. **68:** 3631–3641.
44. **Schnell, M. J., L. Buonocore, E. Kretzchmar, E. Johnson, and J. K. Rose.** 1996. Foreign glycoproteins expressed from recombinant vesicular stomatitis viruses are incorporated efficiently into virus particles. Proc. Natl. Acad. Sci. USA **93:**11359–11365.
45. **Selby, M. J., E. Glazer, F. Masiarz, and M. Houghton.** 1994. Complex processing and protein:protein interactions in the E2:NS2 region of HCV. Virology **204:**114–122.
46. **Selby, M. J., Q.-L. Choo, K. Berger, G. Kuo, E. Glazer, M. Eckart, C. Lee, D. Chien, C. Kuo, and M. Houghton.** 1993. Expression, identification and subcellular localization of the proteins encoded by the hepatitis C viral genome. J. Gen. Virol. **74:**1103–1113.
47. **Spaete, R. R., D. A. Alexander, M. E. Rugroden, Q.-L. Choo, K. Berger, K. Crawford, C. Kuo, S. Leng, C. Lee, R. Ralston, K. Thudium, J. W. Tung, G. Kuo, and M. Houghton.** 1992. Characterization of the hepatitis C virus E2/NS1 gene product expressed in mammalian cells. Virology **188:**819–830.
48. **Stadler, K., S. L. Allison, J. Schalich, and F. X. Heinz.** 1997. Proteolytic activation of tick-borne encephalitis virus by furin. J. Virol. **71:**8475–8481.
49. **Stegmann, T., S. Nir, and J. Wilschut.** 1989. Membrane fusion activity of influenza virus. Effects of gangliosides and negatively charged phospholipids in target liposomes. Biochemistry **28:**1698–1704.
50. **White, J. M.** 1990. Viral and cellular membrane fusion proteins. Annu. Rev. Physiol. **52:**675–697.
51. **Zhang, L., and H. P. Ghosh.** 1994. Characterization of the putative fusogenic domain in vesicular stomatitis virus glycoprotein G. J. Virol. **68:**2186–2193.
52. **Zhou, Y., M. König, G. Hobom, and E. Neumeier.** 1998. Membrane-anchored incorporation of a foreign protein in recombinant influenza virions. Virology **246:**83–94.

NCBI PubMed www.pubmed.gov

A service of the National Library of Medicine
and the National Institutes of Health

My NCBI
[Sign In] [Regis

All Databases PubMed Nucleotide Protein Genome Structure OMIM PMC Journals Boo

Search PubMed for Go Clear

☑ Limits Preview/Index History Clipboard Details

Field: **Title/Abstract**

Display AbstractPlus Show 20 Sort By Send to

All: 1 Review: 1

1: IUBMB Life. 1999 Aug;48(2):151-6. Links

Evolutionary conservation of the membrane fusion machine.

Poumbourios P, **Center RJ**, **Wilson KA**, **Kemp BE**, **Kobe B**.

St. Vincent's Institute of Medical Research, Fitzroy, Victoria, Australia.

Recent structural studies of proteins mediating membrane fusion reveal intriguing similarities between diverse viral and mammalian systems. Particularly striking is the close similarity between the transmembrane envelope glycoproteins from the retrovirus HTLV-1 and the filovirus Ebola. These similarities suggest similar mechanisms of membrane fusion. The model that fits most currently available data suggests fusion activation in viral systems is driven by a symmetrical conformational change triggered by an activation event such as receptor binding or a pH change. The mammalian vesicle fusion mediated by the SNARE protein complex most likely occurs by a similar mechanism but without symmetry constraints.

PMID: 10794590 [PubMed - indexed for MEDLINE]

Related Links

Structural basis for coronavirus-mediated membrane fusion. Crystal structure of mouse hepatitis virus spike protein fusion co [J Biol Chem. 2004]

New insights into the mechanism of virus-induced membrane fusion. [Trends Biochem Sci. 2002]

Definition of an amino-terminal domain of the human T-cell leukemia virus type 1 envelope surface unit that extends the fusogenic range of an ecotropic murine leuk [J Biol Chem. 2000]

The Role of histidine residues in low-pH-mediated viral membrane fusion. [Structure. 2006]

What studies of fusion peptides tell us about viral envelope glycoprotein-mediated membrane fusion (review). [Mol Membr Biol. 1997]

See all Related Articles...

Display AbstractPlus Show 20 Sort By Send to

Write to the Help Desk
NCBI | NLM | NIH
Department of Health & Human Services
Privacy Statement | Freedom of Information Act | Disclaimer

Virology. 1999 Aug 15;261(1):133-42. ELSEVIER FULL-TEXT ARTICLE Links

Fusogenic activity of hepadnavirus peptides corresponding to sequences downstream of the putative cleavage site.

Rodríguez-Crespo I, Núñez E, Yélamos B, Gómez-Gutiérrez J, Albar JP, Peterson DL, Gavilanes F.

Facultad de Ciencias Químicas, Universidad Complutense, Madrid, 28040, Spain.

Sequence homology between the amino-terminal region of the S protein of hepatitis B Virus (HBV) and known fusion peptides from retroviruses and paramyxoviruses led us to propose that this region might be equally involved in the initial infective steps of hepadnaviruses. In fact, we showed that a synthetic peptide corresponding to the N-terminus region of the S protein of HBV had membrane-interacting properties and was able to induce liposome fusion adopting an extended (beta-sheet) conformation (Rodríguez-Crespo et al., 1996, 1995). We describe herein studies on the interaction of peptides derived from the N-terminal region of the S protein of duck (DHBV: Met-Ser-Gly-Thr-Phe-Gly-Gly-Ile-Leu-Ala-Gly-Leu-Ile-Gly-Leu-Leu) and woodchuck hepatitis B viruses (WHV: Met-Ser-Pro-Ser-Ser-Leu-Leu-Gly-Leu-Leu-Ala-Gly-Leu-Gln-Val-Val) with liposomes. These peptides were able to induce to a different extent aggregation, lipid mixing, and leakage of internal aqueous contents from both neutral and negatively charged phospholipid vesicles in a concentration-dependent and pH-independent manner. Fluorescence depolarization of 1,6-diphenyl-1,3,5-hexatriene-labeled vesicles indicated that both peptides become inserted into the hydrophobic core of the lipid bilayer. Circular dichroism studies indicated that the DHBV peptide adopts an extended conformation in the presence of lipids, whereas the WHV peptide displays a high content of alpha-helical conformation. Therefore, these results extend our previous findings obtained for human hepatitis B virus to other members of the hepadnavirus family and suggest that this region of the S protein is important in the initial steps of the infective cycle. Copyright 1999 Academic Press.

PMID: 10441561 [PubMed - indexed for MEDLINE]

: Virus Res. 2000 Jun;68(1):35-49. ELSEVIER FULL-TEXT ARTICLE Links

Hemifusion activity of a chimeric influenza virus hemagglutinin with a putative fusion peptide from hepatitis B virus.

Berting A, Fischer C, Schaefer S, Garten W, Klenk HD, Gerlich WH.

Institut für Virologie, Philipps Universität, Marburg, Germany.

Entry of enveloped viruses is often mediated by an aminoterminal hydrophobic fusion peptide of a viral surface protein. The S domain of the hepatitis B virus surface protein contains a putative fusion peptide at position 7-18, but no systems are available to study its function directly. We tested the functionality of this peptide and a related peptide from another hepadnavirus in the context of the well-characterized influenza virus hemagglutinin H7 using gene mutation. The chimeric hemagglutinins could be expressed stably in CV 1 cells and were transported to the cell surface. The chimeras were incompletely cleaved by cellular proteases but cleavage could be completed by trypsin treatment of the cells. The chimeras did not differ in receptor binding, i.e. erythrocyte binding. Hemifusion and fusion pore formation were detected with membrane or cytosolic fluorescent dye-labeled erythrocytes as target structures of the hemagglutinin. Five of six different chimeras mediated hemifusion in 20-54% of the hemagglutinin-expressing cells, complete fusion and syncytium formation was not observed. The data suggest that the sequence 7-18 of the hepatitis B S domain may indeed initiate the first step of viral entry, i.e. hemifusion.

PMID: 10930661 [PubMed - indexed for MEDLINE]